Master's thesis

NTNU
Norwegian University of Science and Technology
Faculty of Natural Sciences
Department of Energy and Process Engineering

Ida Havnen Ullsfoss

Modeling Thermal Degradation of Monoethanolamine

Master's thesis in MTKJ
Supervisor: Hanna Knuutila
Co-supervisor: Lucas Braakhuis
June 2021

NTNU
Norwegian University of
Science and Technology

Ida Havnen Ullsfoss

Modeling Thermal Degradation of Monoethanolamine

Master's thesis in MTKJ
Supervisor: Hanna Knuutila
Co-supervisor: Lucas Braakhuis
June 2021

Norwegian University of Science and Technology
Faculty of Natural Sciences
Department of Energy and Process Engineering

NTNU
Norwegian University of
Science and Technology

Abstract

Background: Thermal degradation of Monoethanolamine (MEA) is an unfortunate aspect of the process of post-combustion capture (PCC) as it leads to loss of solvent and decreased solvent absorption capacity of CO_2. The stripper conditions are limited to restrain the occurrence of thermal degradation, and a better understanding of the degradation would enable a more precise optimization of the stripper conditions. This thesis aimed to increase the knowledge on thermal degradation by making a model that can predict the loss of solvent and the formation of degradation products as a function of the stripper conditions.

Method: A model describing thermal degradation as a function of temperature and CO_2 loading was found in literature and successfully recreated. The considered degradation products were HEIA, HEEDA, Trimer, and TriHEIA. The included data set was enlarged to evaluate the model at extended ranges of temperatures and CO_2 loadings. By the addition of data, the total error of the model predictions was found to increase significantly. An optimization routine was therefore added to the model to improve the fit to the complete data set. Particle swarm optimization was used to minimize the total root mean squared error (RMSE) between the modeled and experimental values, and a new set of parameters was found for the rate equations in the kinetic model. The RMSE was preferred as the objective function to accentuate the fitting of MEA, which is the most critical to predict.

Conclusion: By optimization, the total RMSE decreased by 30% from the original model, caused by improved descriptions of the three most significant components, MEA, HEEDA, and HEIA. The final model provided adequate estimations of the experimental concentration profiles of MEA, as the associated average relative error was found to be 5%. Contrary, deficiencies in the fittings of the degradation products were reflected in average relative errors ranging from about 70 to 77%. The significant deviations are considered a result of the prioritized fitting of MEA, differences in the provided experimental data at the same experimental conditions, and general uncertainty related to the applied kinetic model. Despite the inefficiencies in describing the degradation products, the model is considered a good starting point for further model development.

Sammendrag

Bakgrunn: Termisk degradering av monoetanolamin (MEA) er et ugunstig aspekt ved aminbasert karbonfangst, da det medfører tap av MEA og redusert absorpsjonskapasitet av CO_2. Temperaturen i stripperen justeres for å begrense forekomsten av termisk degradering, og en bedre forståelse av nedbrytningen muliggjør en mer presis optimalisering av stripperforholdene. Målet med denne oppgaven er å øke kunnskapen om termisk nedbrytning ved å lage en modell som kan forutsi tap av MEA og dannelse av nedbrytningsprodukter, som en funksjon av forholdene i stripperen.

Metode: En allerede eksisterende modell som beskriver termisk degradering, som en funksjon av temperatur og startkonsentrasjon av CO_2, ble rekonstruert. Datasettet ble utvidet for å kunne vurdere modellpresisjonen for et økt antall datapunkter, temperaturer og startkonsentrasjoner av CO_2. Den totale prediksjonsfeilen i modellen økte betydelig ved utvidelse av datasettet. En optimaliseringsrutine ble derfor tillagt modellen for å forbedre tilpasningen til det fulle datasettet. Optimalisering ble utført ved hjelp av 'standard particle swarm optimization', ved å minimere den totale rot-gjennomsnittlige kvadrerte feilen (RMSE) mellom de predikterte og de eksperimentelle verdiene. Dermed ble et nytt sett med parametere funnet for hastighetsligningene i den kinetiske modellen. RMSE ble foretrukket som objektfunksjon, da den fremmer tilpasningen av MEA, som dessuten er den mest kritiske komponenten å prediktere.

Konklusjon: Optimaliseringen reduserte den totale RMSE-verdien med 30% fra den originale modellen, forårsaket av prediksjonsforbedringene av MEA, HEEDA og HEIA. Den endelige modellen ga en presis beskrivelse av de eksperimentelle verdiene for MEA, med et gjennomsnittlig relativt avvik på 5%. De tilsvarende avvikene for nedbrytningsproduktene ble betydelig høyere, og varierte fra ca. 70 til 77 %. Dette regnes som et resultat av at tilpasningen til MEA prioriteres under optimaliseringen, forskjeller i de tilgjengelige eksperimentelle dataene, som vanskeliggjør tilpasningene, og generell usikkerhet knyttet til validiteten av den kinetiske modellen.

Preface

This master's thesis have been carried out at the Department of Chemical Engineering at the Norwegian University of Science and Technology during the spring of 2021.

I would like to thank my supervisor Hanna Knuutila for valuable help and guidance throughout the thesis. I would also like to thank my co-supervisor, Lucas Braakhuis, for his positivity, his constant willingness to help and particularly for the support and advice related to the modeling part of the thesis. Vanja Buvik also deserves a thank for always bringing a positive spirit and for valuable help in academic discussions.

I would also like to give a special thanks to my cohort during this pandemic, for the general encouragement and support.

I declare that this is an independent work according to the exam regulations of the Norwegian University of Science and Technology.

Trondheim, June 25, 2021

Ida Havnen Ullsfoss

Contents

List of Figures

List of Tables

Nomenclature

A	Pre-exponential factor [L $mol^{-1} day^{-1}$]
C	Concentration [mol L^{-1}]
E	Error [mol L^{-1}]
Ea	Activation Energy [J] or [Kcal mol^{-1}]
k_{ref}	Reference Rate Constant[L $mol^{-1} day^{-1}$]
k	Forward Rate Constant [L $mol^{-1} day^{-1}$]
k	Reverse Rate Constant [L $mol^{-1} day^{-1}$]
m	Reaction order
N	Number of reactants
n	Number of points
p	Number of parameters
R	Gas constant [J K^{-1} mol^{-1}]
$RMSE$	Root Mean Squared Error [mol L^{-1}]
T_{ref}	Reference Temperature [K] or [°C]
T	Temperature [K] or [°C]

Chapter 1

Introduction

1.1 Climate change and greenhouse gas emissions

Global warming is a fact, and it is one of the worlds most pressing challenges. Human activities have caused an accumulation of heat-trapping greenhouse gases in the atmosphere, which have caused a rise of the temperature on earth. According to NASA [7], the global temperature has increased by about 1°C since the pre-industrial period, and the current trend indicates a continuous increase of 0.2°C every decade. Elevation of the average temperature is expected to entail changes of ecosystems, increased frequency of extreme weathers, rise of sea levels, and melting of ice in the poles and on glaciers.

A major contributor to global warming is anthropogenic emissions of CO_2, mainly caused by fossil fuel burning. Since the beginning of the industrial revolution, the atmospheric concentration of CO_2 has increased by 47% [8]. A uniform understanding of the seriousness of the emissions has caused an acceleration in the development of renewable energy sources. However, the research and implementation of such technologies are time-consuming, and in the meantime, the world is heavily dependent on fossil fuels. It is, therefore, crucial to make cuts in the current emissions from the existing energy plants. Carbon Capture, Utilization, and Storage (CCUS) has been introduced as an important emissions reduction technology. CCUS involves capturing CO_2 from flue gas in combustion processes, transportation of the CO_2, and either reuse of the CO_2 or storage underground in geological formations.

1.2 Post Combustion Capture

An effective CO_2 capture process is post combustion capture (PCC). This process involves removing the CO_2 by utilizing advanced sorbent, solvent, and membrane systems, or combinations of the different technologies. However, the most common technology for PCC is chemical absorption using aqueous alkanolamine solutions. The most customary amine sorbent is monoethanolamine (MEA) due to its advantageous properties, such as fast kinetics, high absorption capacity, low price, and high water solubility [9]. Figure 1.2.1 shows a typical PPC-process, where MEA is used as sorbent.

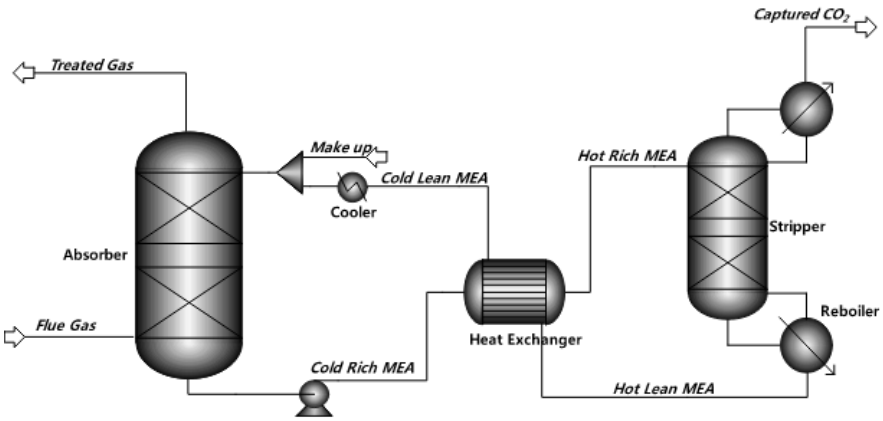

Figure 1.2.1: Flowsheet of a typical amine based CO_2 capture process [1].

Flue gas with around 10% CO_2 enters the bottom of the absorber column after being cleaned from fly ash and sulfur and cooled to about 40°C. The gas flows upwards and contacts counter-currently with CO_2-lean amine solution. The lean amine solution typically contains 15-40wt% MEA and 0.2-0.4 moles CO_2 per mole MEA [5]. The low absorber temperature of about 40-70°C ensures a high affinity of CO_2, and causes most of the CO_2 from the flue gas to be absorbed by MEA. Typically, more than 85% of the CO_2 is removed from the flue gas [10]. The purified flue gas is then released from the absorption tower. The CO_2-rich stream is transported from the bottom of the absorber column into a heat-exchanger, where it is preheated by the hot lean MEA solution that exits the reboiler. The heated CO_2-rich stream then enters the stripper head and flows down the column. Steam is generated from the reboiler at the bottom of the stripper and flows counter currently to the CO_2 rich MEA solution. As the CO_2 rich MEA solution contacts with the counter flowing steam, the affinity of CO_2 decreases, and the CO_2 desorbs by temperature swing. Released CO_2 follows the ascending steam out of the stripper head and into the condenser. Condensed steam is directed back into the stripper as reflux, and gas of about 99% clean CO_2 gas is released from the

system for further sequestration and transport. The regenerated absorption liquid in the reboiler is then recycled back into the absorber head.

1.3 Degradation

A challenge related to the amine-based CO_2 capture process is that the absorption capacity of CO_2 is reduced with time. The reduction is explained by solvent degradation through irreversible side reactions with CO_2, oxygen, SOx, and NOx [11]. Byproducts lead to a significant decrease in the process efficiency due to solvent losses, corrosion, foaming, fouling, and an increase in viscosity [12]. Additional operating costs are generated by the demand for solvent replacement and removal of corrosive and volatile degradation products from the solvent. In fact, the operating costs related to amine degradation have been estimated to be around 10% of the total CO_2 capture cost [13].

The main degradation pathways in the amine-based absorption system are oxidative and thermal degradation. Oxidative degradation mainly occurs in the absorber due to the high relative concentration of oxygen, which is introduced by the flue gas. Thermal degradation mainly occurs in the desorption of CO_2, and is classified into carbamate polymerization and thermal degradation. Carbamate polymerization is the reaction pathway catalyzed by CO_2, and thermal degradation occurs at temperatures above 205°C. This thesis mainly focuses on thermal degradation by carbamate polymerization.

1.4 Impact of Thermal Degradation on Energy Requirement

Thermal degradation is strongly temperature dependent [14]. According to Rochelle [15], the occurrence of thermal degradation in the stripper would be insignificant if the temperature and liquid holdup in the stripper bottom was reduced. However, the overall energy requirement and costs of the stripper and compressor are reduced at elevated pressure and temperature [16,17].

The purified CO_2 gas that leaves the stripper head is compressed before further transport. By increasing the temperature in the stripper, CO_2 is thermally compressed before leaving the stripper. The requirement and cost of mechanical compression are thereby reduced. Additionally, increased temperature streamlines the amine recovery and increases the CO_2-steam ratio, which enhances the efficiency of the reboiler

energy. Consequently, the size of the stripper and the related capital costs are reduced. Rochelle [15] performed a study proving that, for a single heated flash, an increase from 90 to 150°C, reduced the equivalent work by 30%. In other words, there is potential for increased efficiency and economic savings by elevating the pressure and temperature in the stripper.

The reduced energy requirement and increased occurrence of thermal degradation by elevating the stripper temperature results in an optimization problem between maintenance of the solvent and the energy efficiency.

1.5 Objective

The chemistry of thermal degradation and the pathways of the formations of degradation products are not yet fully understood and require further research. Knowledge of the mechanisms and the effect of the process parameters would be advantageous in developing new stripper configurations, which, according to Davis [5], is the most significant economic factor in the capture of CO_2. In order to find the optimal stripper conditions, a precise model of thermal degradation needs to be developed as a function of the stripper conditions.

The objective of this master's thesis was to obtain a better understanding of thermal degradation by making a model that can predict the loss of MEA and the formation of degradation products for varying temperatures and initial CO_2 loadings. Therefore, a full kinetic model describing the degradation pathway was required, with the inclusion of the dependency of temperature and initial CO_2 loading. A suited kinetic model was developed by Davis [5]. In the work by Davis, the model was fitted to the experimental data from the experiments performed in the same study. In this work, the model by Davis was recreated, and its ability to represent other thermal degradation data sets was evaluated. A self-constructed optimization routine was then implemented in order to find the optimal model parameters to describe the entire data set.

1.6 Structure

The thesis is divided into four parts. The first part (I) includes the theoretical background necessary to understand the mechanism of thermal degradation and the experiments behind the experimental data, which is used as the basis in the modeling. The second part (II) covers all information relevant to the model development. This includes the details of Davis' model, the recreation of the model, and the procedure behind making the final model. Part three (III) ties the two previous parts together by providing the results along with a thorough discussion. Finally, part four (IV) sums up the results and provides recommendations for further work.

Part I

Theoretical Background

Chapter 2

Thermal Degradation

2.1 Thermal Degradation

The rate of thermal degradation of alkanoamines from carbamate polymerization limits the stripper to operate at 100–130°C, and most strippers in industrial carbon capture plants are operated with a maximum temperature of 120°C [18]. According to Rochelle [15], thermal degradation only takes place at temperatures above 205°C. Since this temperature is above the temperature range used in amine-based CO_2 capture plants, thermal degradation due to high temperatures will not be further discussed in this thesis.

2.2 Carbamate polymerization

In amine-based CO_2 capture plants, absorption of CO_2 mainly occurs in the absorber. CO_2 can dissolve into the solvent by physical absorption but is mainly absorbed through chemical reactions with MEA. MEA is a primary amine that acts as a weak base and reacts with weak acids such as CO_2 at ambient temperatures. The chemical absorption of CO_2 involves many reactions, but there are two fundamental mechanisms [19], shown in the reactions in Figure 2.2.1 and 2.2.2.

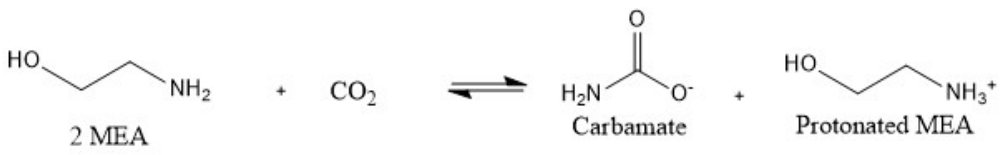

Figure 2.2.1: Absorption of CO_2 by formation of carbamate.

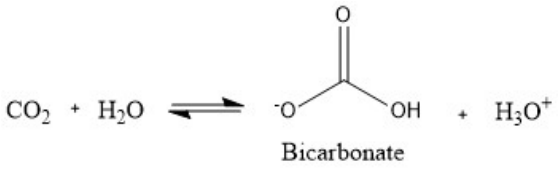

Figure 2.2.2: Absorption of CO_2 by formation of bicarbonate.

In the reaction in Figure 2.2.1, CO_2 and MEA reacts to form stable carbamate molecules. Some CO_2 can also react with water to form bicarbonate, as shown in Figure 2.2.2 [19]. However, the absorption of CO_2 is mainly caused by the formation of carbamate at the relevant concentrations of CO_2 [20].

The concentration of CO_2 is commonly given as CO_2 loading, which expresses the number of moles of CO_2 absorbed per mol of MEA. Further, the maximum loading is referred to as the absorbing capacity of a solvent. As illustrated in Figure 2.2.1, two moles of MEA molecules are required to absorb one mole of CO_2 due to the formation of the protonated MEA molecule. By stochiometry, the absorption capacity of MEA is therefore 0.5 moles CO_2 per mole of MEA.

At elevated temperatures, the reactions of absorption in Figure 2.2.1 and 2.2.2 are usually reversed. However, this is not always the case, as the involved components can participate in further reactions. A major disadvantage of using alkanolamines is their tendency to react with other components than the acid gas. MEA can participate in irreversible degradation processes where the product is unable to absorb CO_2. In other words, these reactions cause a loss of MEA and a reduction of the absorption capacity [21].

2.3 Pathway of Carbamate Polymerization

The main mechanism for thermal degradation of MEA in an absorber/stripper system is carbamate polymerization [5, 14, 22]. The pathway of carbamate polymerization is quite complex, and there are uncertainties related to the exact details of the mechanism. Polderman [2] was the first to propose a detailed reaction pathway. Since then, several researchers have suggested pathways that differ from the mechanism presented by Polderman [2]. Some of these proposals are discussed in the following sections.

2.3.1 Polderman

According to Polderman et al. [2], MEA carbamate, formed in the reaction in Figure 2.2.1, cyclizes to form oxazolidone (OZD) in a dehydration reaction. Oxazolidone reacts with MEA to form 1-(2-hydroxyethyl)-2-imidazolidone (HEIA). HEIA is considered an immediate product, as it reacts further with water to form N-(2-hydroxyethyl)-ethylenediamine (HEEDA). The complete degradation pathway is shown in Figure 2.3.1.

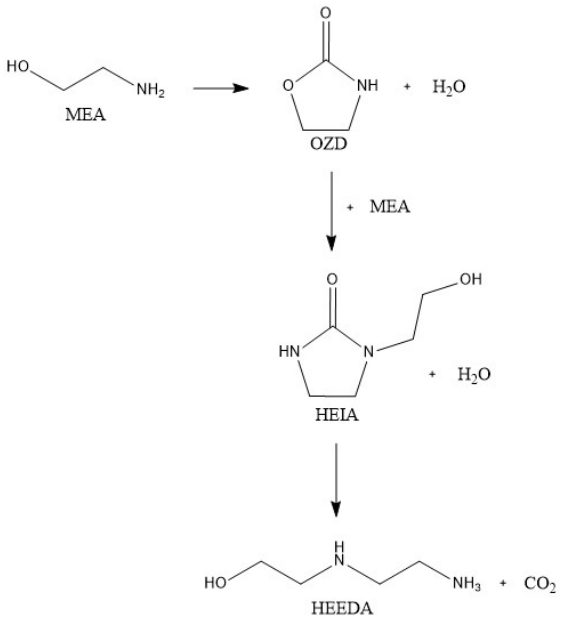

Figure 2.3.1: Thermal Degradation Pathway proposed by Polderman et al. [2].

2.3.2 Yazvikova

Yazvikova et al. [3] proposed another pathway of MEA degradation in a study performed at 200°C, which is significantly higher than applied by the other researchers. The study was the first to introduce N,N'-di(hydroxyethyl)urea (MEA Urea) as a product from the reaction between OZD and MEA. This step was not present in the pathway by Polderman et al. [2]. Further, Yazvikova et al. [3] reports that MEA Urea converts into HEIA and further hydrolyses to HEEDA, which is proposed as the final degradation product. The order of HEIA and HEEDA formation agrees to the pathway by Polderman et al [2]. Figure 2.3.2 illustrates the entire pathway suggested by Yazvikova et al [3].

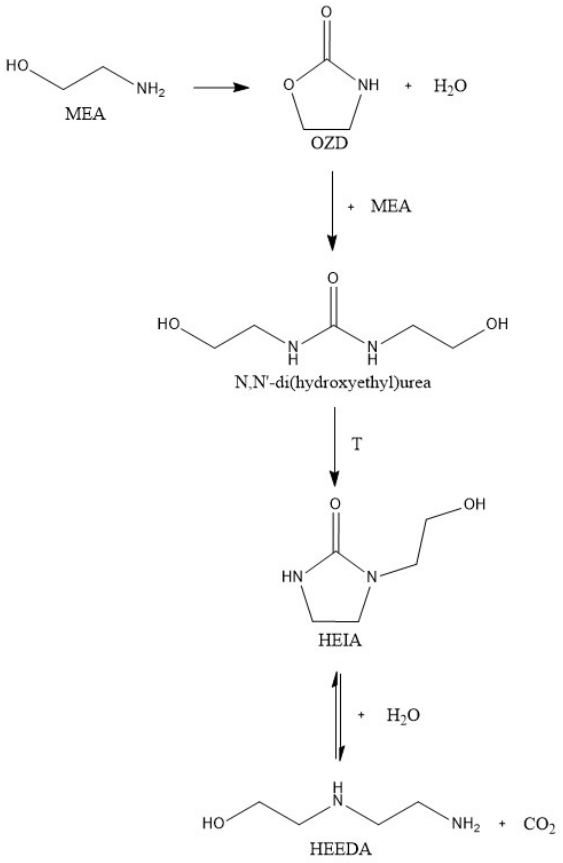

Figure 2.3.2: Thermal Degradation Pathway proposed by Yazvikova et al [3].

It must be noted that this experiment was performed in the absence of water. Water dilutes MEA, affects the energy of solvation, and is likely to take part in several reactions as a proton acceptor or donor. In consequence, water is expected to impact the occurring degradation reactions.

2.3.3 Lepaumier

Lepaumier et al. [4] reported a third option for the reaction between OZD and MEA, where HEEDA is formed. HEEDA then reacts with water to form HEIA. This step is opposite from what was suggested by Polderman et al. [2] and Yazvikova et al. [3], where HEEDA was formed from HEIA. HEEDA reacts further with OZD to form MEA Trimer, which reacts with CO2 and forms 1-(2-aminoethyl)-3-(2-hydroxyethyl)imidazolidin-2-one (AEHEIA). Figure 2.3.2 summarizes the reactions.

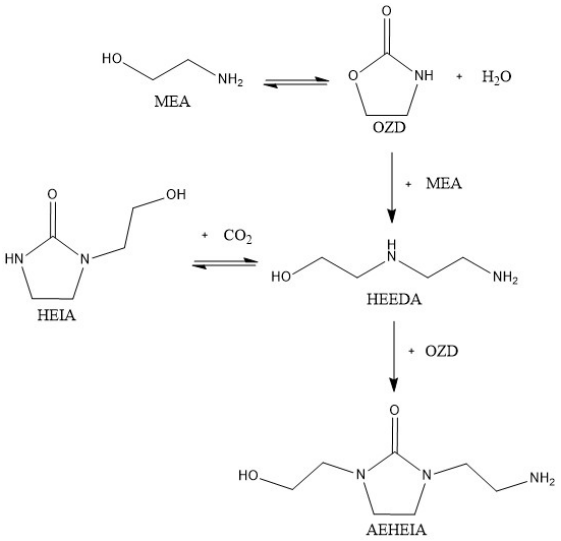

Figure 2.3.3: Thermal Degradation Pathway proposed by Lepaumier et al [4].

This reaction pathway is in accordance with the pathway suggested by Davis [5], which is described in Section 3.1, and confirmed by Eide-Haugmo [21]. As opposed to Davis [5], Lepaumier et al. [4] and Eide-Haugmo [21] detected AEHEIA, and not triHEIA.

To summarize, the discussed studies agree that the mechanism of thermal degradation is carbamate polymerization. Some of the earliest studies suggested HEIA as the precursor for HEEDA. More recent studies agree on the contrary. There is also a consensus that the major degradation products are HEIA and HEEDA, of which HEIA is the most stable degradation product. The researchers also agree that the first and critical product causing MEA deactivation is OZD.

2.4 Thermal Degradation Experiments

Thermal degradation in industrial plants occurs at a slow rate. Experiments performed at the corresponding temperatures will therefore be time-consuming and requires months or years. Elevated temperatures and pressures are therefore used during the experiments in order to speed up the process.

2.4.1 A typical Experiment

There are some variations in the experimental procedures, but they all follow the same general approach. Initially, the solutions are prepared gravimetrically by mixing MEA and deionized water until the target weight percent of MEA. Next, pressurized CO_2 is bubbled through the solutions, and the loading is determined by weight or

liquid analyses. The solutions are filled in cylinders and placed into sealed convection ovens that ensure a constant temperature throughout the experiment. By changing one parameter at a time and keeping the others constant, the impact of the targeted parameters on the occurring degradation is investigated. Typically, the effect of initial CO_2 loading and temperature are studied. At certain time intervals, samples are taken out for analysis, revealing the loss of absorbent and the formation of degradation products. The analyzes indicate how thermal degradation varies as a function of time and reactor conditions.

2.4.2 Analytical Methods

Several analytical methods are used to analyze the degradation samples. However, the main methods are variants of gas chromatography (GC)- coupled with mass spectrometry (MS), and liquid chromatography (LC) coupled with -MS. High-Performance LC (HPLC) is also commonly used method that uses a higher pressure to reduce the time of separation but is essentially the same as LC. During chromatography, the components are carried by a mobile phase, which is a gas for GC and a liquid in LC, through a column covered by the stationary phase, which enables separation of the components. Dependent on the choice of stationary phase, the components are separated based on their physical or chemical properties, such as i.e., size and/or polarity. The separated compounds are sent through a mass spectrometer. By ionizing chemical compounds, the mass spectrometer separates and measures the mass to charge ratio of a molecule ion or the ionic fragments of the molecule. By measuring each compound's time to pass the chromatography column (retention time) and by studying the mass spectrum, the different components can be identified and quantified by calibration with known standards.

Some of the degradation products are commercially unavailable, and the lack of analytical standards complicates the identification and quantification of the degradation compounds. In such cases, the exact structures of the degradation products are determined based on educated guesses by the researchers.

2.5 Literature Review

Davis and Rochelle [14] investigated thermal degradation of MEA at stripper conditions in stainless steel cylinders placed in convection ovens. The initial MEA concentration was 30wt%, the temperature ranged from 100 to 150°C, the CO_2 loading from 0.2-0.5 mol CO_2 per mol MEA and the total duration of the experiments was eight weeks.

The degradation compounds were identified using known addition spiking on IC and HPLC, and mass spectrometry. The result at the lowest investigated CO_2 loading and temperature gave 2% MEA loss, and the highest loading and temperature gave 89% degradation. In another study, Davis [5] performed experiments in the same temperature and loading ranges but extended the duration of the experiments and the frequency of sample analyzes. After 16 weeks with loading 0.4 and 120°C, 29% of the initial MEA had degraded. By using all of the obtained experimental data, a reaction pathway and a full kinetic model were proposed. Integration of the kinetic model resulted in a model describing the loss of MEA and CO_2, and formation of HEEDA, Trimer, Polymeric products, HEIA, and TriHEIA. The details of this model will be presented in Chapter 3.

Leonard et al. [6] quantified the MEA loss and degradation products from a 30wt% MEA solution at 120 and 140°C with an initial CO_2 loading of 0.44. HEEDA, HEIA, and OZD were found to be the main degradation components, and the MEA loss after three weeks was about 5% at 120°C and 37% at 140°C. The experimental data was used to make a simple model, where the irreversible formation of HEIA was considered to cause degradation. The pre-exponential factor and the activation energy of the Arrhenius equation were found by minimizing the sum of the squared difference between modeled and experimental errors. The resulting rate of degradation was $1.19 \cdot 10^{-7}$ mol MEA/Ls at 120°C and $1.02 \cdot 10^{-6}$ mol MEA/Ls at 140°C.

Lepaumier et al. [4] examined degradation in 30wt% MEA solutions, using thermal batch cylinders and a CO_2 loading of 0.5 at 135°C. After five weeks, 57.6% of the MEA was degraded. The rate of degradation was approximately constant for the first four weeks before it started to decrease. LC-MS was used to quantify the remaining amine, and GC-MS was used to identify and quantify the main degradation compounds. The identified degradation products were, in accordance with the reaction pathway in Figure 2.3.3, HEIA, HEEDA, OZD, and the new product, AEHEIA.

Eide-Haugmo [21] performed an experiment with the same experimental conditions as Lepaumier, and the same degradation compounds were detected in this research. Eide-Haugmo found the loss of MEA to be 44% after five weeks, which is lower than seen in the result by Lepaumier.

The experimental apparatus used in the experiment by Zoannou et al. [22] stands out from the rest of the experiments. Whilst the other experiments were performed in closed systems, the experiment by Zoannou was performed in what is considered an open setup. A temperature of 160°C was kept by using high-pressure vessels. After eight weeks, the solutions of 30wt% MEA and initial loadings of 0.19 and 0.37 proved

a decrease of respectively 83 and 95% in MEA concentration. GC–MS was used to detect several degradation products, of which HEEDA, HEIA, and OZD were the main components. In addition, MEA Urea, which Davis previously found, was also identified in small amounts.

Fytianos participated in several studies on the effect of the degradation products on corrosion. As a part of these studies, thermal degradation of 30wt% MEA was investigated. Fytianos et al. [23] found that 38% of the initial MEA was degraded after five weeks at 135°C and with a CO_2 loading of 0.4. HEEDA, HEIA, and OZD were among the detected degradation products; however, only HEIA and HEEDA were measured in significant amounts. These results were consistent in later research by the same author, at the same experimental conditions.

2.6 Parameters that affects thermal degradation

As a result of the experiments performed for thermal degradation of MEA, the loss of MEA is found to be primarily dependent on three factors.

MEA is thermally stable at temperatures up to 100°C, and thermal degradation is insignificant at temperatures below this point [24]. The greatest rate of degradation in amine-based carbon capture plants occurs at 120–150°C [15], and the rate is proven to be highly temperature dependent within this interval. As already mentioned, the increase from 120 to 140°C in the experiment by Leonard [6] increased the degradation by 32%. This experiment is one of many that proves the strong temperature dependency of thermal degradation. Essentially, an increase in temperature from 120°C implies a notable acceleration in the kinetics of carbamate polymerization, and the extent of degradation increase accordingly.

Another factor that is proven to affect the stability of MEA is the presence and concentration of CO_2. In addition to the experiments at stripper conditions, Leonard [6] compared the extent of degradation with and without the presence of CO_2. After three weeks, the degradation of MEA was 5% in the absence of CO_2, and of 38% at a CO_2 loading of 0.44. This observation confirms that the presence of CO_2 has a significant impact on the thermal stability of MEA. Davis and Rochelle [14] also showed escalated degradation by increasing the loading. At 135°C, the loss of MEA after eight weeks increased from 21% to 53% by changing the respective loading from 0.2 to 0.5. Principally, increased CO_2 loading increases the equilibrium concentration of oxazolidone and thereby accelerates the carbamate polymerization.

Davis and Rochelle [14] also state that the initial amine concentration affects the degree

of thermal degradation. In the report by Davis [5], old experiments with varying initial amine concentration are given. The degradation with initial amine concentrations of 2.88, 4.9, and 6.58 mol/L increased with the respective values of 25, 37, and 46%. Subsequently, the rate of degradation was found to increase by the initial amine concentration. With similar reasoning as for CO_2, the observations are explained by an increased equilibrium concentration of the oxazolidone and following increased rate of degradation.

Several other parameters may influence the extent of thermal degradation. However, loading, temperature, and amine concentration are considered the main factors that impact degradation.

Part II

Methodology and Approach

Chapter 3

The Model by Davis

In the work by Davis [5], degradation experiments were performed to measure the amount of MEA loss and formed degradation products. Based on the experimental results, a reaction mechanism was proposed and used as the basis to develop a kinetic model. The model describes the concentrations of MEA and the detected degradation products as a function of temperature, initial MEA concentration, and CO_2 loading. The following sections present the reactions, kinetics, and general approach used in Davis' model.

3.1 Reactions

The reactions considered in the modeling follow the mechanism proposed by Davis [5], already shortly presented in Chapter 2. The reaction mechanism is given by the following steps.

First, CO_2 is absorbed by MEA, forming carbamate and a protonated MEA molecule, shown in Reaction RX1.

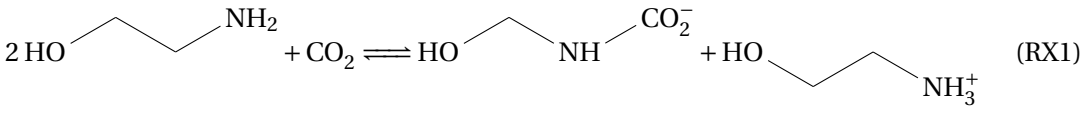

(RX1)

Carbamate reacts with protonated MEA, undergoes a hydrolyze reaction, and forms oxazolidone and MEA, as illustrated in Reaction RX2.

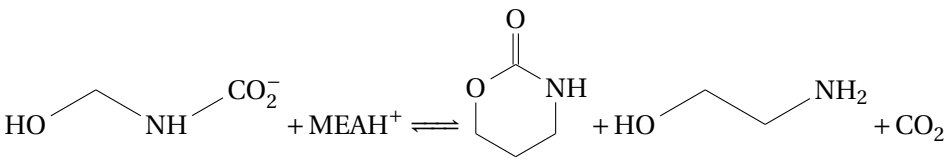

(RX2)

MEA attacks the ketone group of the oxazolidone and forms MEA Urea, which Zoannou also reported. The formation occurs as shown in Reaction RX3.

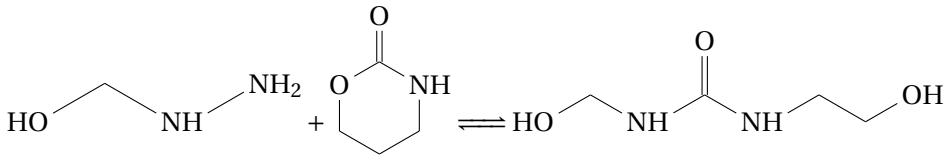

(RX3)

MEA can also attack the oxazolidone molecule from the side, forming N-(2-hydroxyethyl)-ethylenediamine(HEEDA), as shown in Reaction RX4.

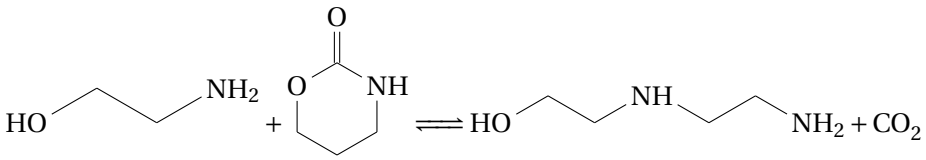

(RX4)

The HEEDA molecule reacts with CO_2 and cyclizes into hydroxyethyl-imidazolidone(HEIA), as shown in Reaction RX5.

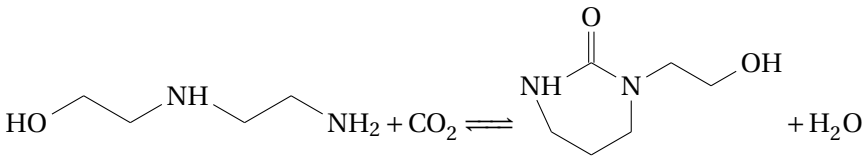

(RX5)

This means that, according to the study by Davis, HEIA is formed from HEEDA. As already mentioned, this order of formation corresponds to the pathway reported by Lepaumier [4] and Eide-Haugmo [21] but contradicts the results by Polderman [2] and Yazvikova [3], where HEIA is a precursor to HEEDA.

The Oxazolidone molecule can be attacked by HEEDA and form more MEA Urea, or it can continue the polymerization reaction to form (N-(2-hydroxyethyl)-diethylenetriamine), which is referred to as the trimer of MEA. This occurs by the reaction given in Reaction RX6.

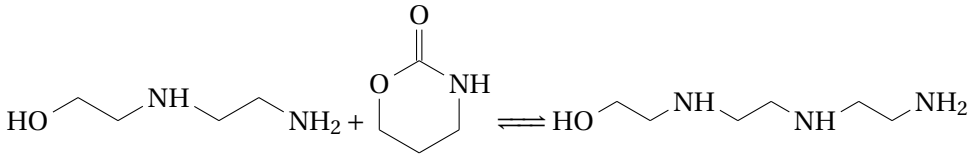

(RX6)

By further reaction with CO_2, MEA Trimer can form cyclic urea of MEA Trimer, 1-[2-[(2-hydroxyethyl)amino]ethyl]-2-imidazolidone, as shown in Reaction RX7.

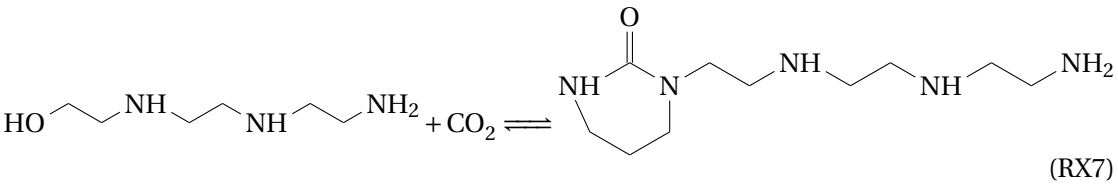

(RX7)

With evidence in the experiments, this polymerization reaction can continue indefinitely through the quatramer of MEA, N-(2-hydroxyethyl)triethylenetetramine, and the corresponding cyclic urea, 1-[2-[[2-[(2-hydroxyethyl)amino]ethyl]amino)ethyl]-2-imidazolidone [5].

To summarize the above reactions, an overview of the reaction pathway suggested by Davis is encapsulated in Figure 3.1.1.

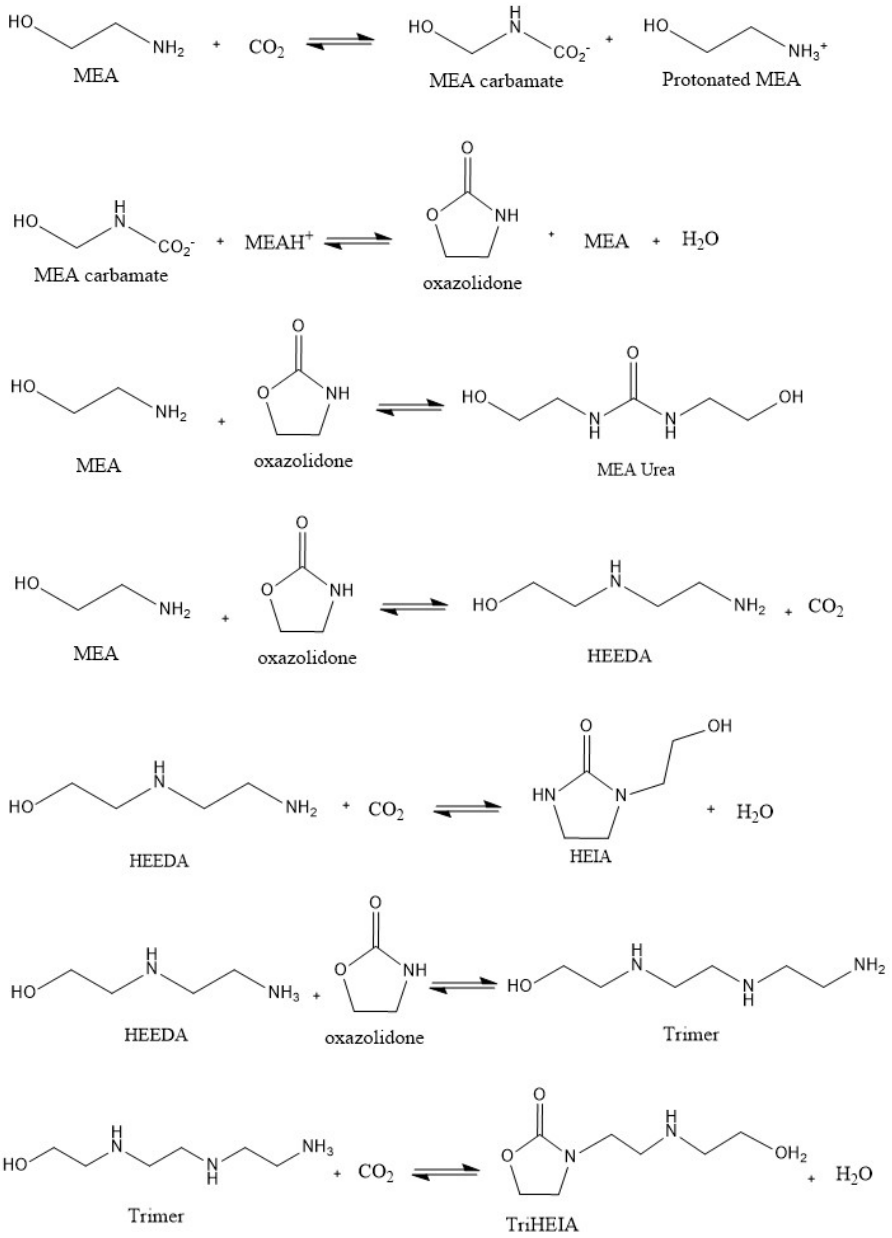

Figure 3.1.1: Thermal Degradation Pathway proposed by Davis [5].

3.2 Kinetic Model

Davis proposed a kinetic model by applying the rate law to the reactions involved in the degradation pathway. The rate law relates the rate of a chemical reaction and the concentration of its reactants, as shown in Equation 3.2.1.

$$\frac{dC}{dt} = k\prod_{i=1}^{N} C_i^{m_i} - k_{-}\prod_{i=1}^{N} C_i^{m_i} \tag{3.2.1}$$

Where k and k_{-} are the reaction rate coefficients for the equilibrium's respective forward and reverse reaction. N is the number of reactants, C_i is the concentration of reactant i, and m is the reaction order of the reactants.

Combination of the rate laws for the degradation reactions resulted in a set of ordinary differential equations (ODEs), listed in Equation 3.2.2-3.2.8.

$$\frac{d[MEA]}{dt} = -k_1 2[MEA][CO_2] - k_2[HEEDA][CO_2] - k3[Trimer][CO_2] \tag{3.2.2}$$

$$\frac{d[HEEDA]}{dt} = k_1[MEA][CO_2] - k_2[HEEDA][CO_2] - k_4[HEEDA][CO_2] + k_{-4}[HEIA] \tag{3.2.3}$$

$$\frac{d[Trimer]}{dt} = k_2[HEEDA][CO_2] - k_3[Trimer][CO_2] - k_5[Trimer][CO_2] + k_{-5}[triHEIA] \tag{3.2.4}$$

$$\frac{d[Poly]}{dt} = k_3[Trimer][CO_2] \tag{3.2.5}$$

$$\frac{d[HEIA]}{dt} = k_4[HEEDA][CO_2] - k_{-4}[HEIA] \tag{3.2.6}$$

$$\frac{d[TriHEIA]}{dt} = k_5[Trimer][CO_2] - k_{-5}[TriHEIA] \tag{3.2.7}$$

$$\frac{d[CO_2]}{dt} = k_{-4}[HEIA] - k_4[HEEDA][CO_2] + k_{-5}[TriHEIA] - k_5[Trimer][CO_2] \tag{3.2.8}$$

Each rate constant, k_i, incorporated in the kinetic model above, corresponds to different reactions from the degradation pathway. The link between the rate constants and the described reaction is outlined below.

k1 = rate constant for conversion of MEA and Oxazolidone to HEEDA ($L \cdot mol^{-1} hr^{-1}$)
k2 = rate constant for conversion of HEEDA and Oxazolidone to MEA Trimer ($L \cdot mol^{-1} hr^{-1}$)
k3 = rate constant for conversion of MEA Trimer and Oxazolidone to polymeric products ($L \cdot mol^{-1} hr^{-1}$)
k4 = rate constant for conversion of HEEDA carbamate to HEIA ($L \cdot mol^{-1} hr^{-1}$)
k_{-4} *= rate constant for conversion of HEIA to HEEDA carbamate* (hr^{-1})
k5 = rate constant for conversion of MEA Trimer carbamate to TriHEIA ($L \cdot mol^{-1} hr^{-1}$)
k_{-5} *= rate constant for conversion of TriHEIA to MEA Trimer carbamate* (hr^{-1})

Equation 3.2.3-3.2.8 define the formation of polymeric products of MEA. From the reaction mechanism in Figure 3.1.1, oxazolidone is seen to act as a reactant in the vast majority of the reactions. However, its concentration is omitted from the kinetic model. Davis highlights the difficulty in measuring the concentration of oxazolidone due to its role as an intermediate product. An alternative approach was therefore used to include the oxazolidone concentration in the kinetic model. As illustrated in Reaction RX2, oxazolidone is in equilibrium with carbamate, and carbamate is a product of the reaction between MEA and CO_2. Most of the available CO_2 is consumed in the formation of carbamate, and the concentrations of carbamate CO_2 are therefore closely related. By this argument, Davis used the concentration of CO_2, combined with the rate constant, as a surrogate for the oxazolidone concentration in the kinetic model.

Davis' reaction pathway includes the formation of further polymeric products, which encompass quatramer and larger polymeric. Due to sparse data, the formation of such polymeric products was lumped together and described by Equation 3.2.5.

3.3 Modeling

MEA participates in most of the reactions involved in the degradation pathway, and there is a lack of truly stable products. Consequently, the differential equations in the kinetic model are linearly dependent and can not be solved analytically. Davis, therefore, solved the set of differential equations by simple numerical integration. The preferred method was Euler's method, and by using small time steps, the ODEs were solved in Microsoft Excel. The rate constants were modified until the sum of the squared differences between the modeled and experimental concentrations were minimized. After determination of the rate constants for all temperatures, the values of the constants were plotted in an Arrhenius plot. The temperature dependency of the rate constants was described by using the Arrhenius equation, which is given in Equation 3.3.1.

$$k = Ae^{-\frac{Ea}{RT}} \tag{3.3.1}$$

Where A is the pre-exponential factor, E_a is the activation energy, R is the gas constant, and T is the temperature.

By taking the slope from the Arrhenius plot, the pre-exponential constants and activation energies were found. The resulting parameter values are listed in Table 3.3.1.

Table 3.3.1: The optimal pre-exponential constants and activation energies found by Davis [5]. *Parameter values assumed by Davis.

Rate constant	**Pre Exponential Constant** [L day^{-1} mol^{-1}]	**Activation Energy** [kcal/mol]
k_1	1.05 E16	34.4
k_2	2.15 E16	33.3
k_3	3.28 E15	31.5
k_4	3.58 E16	33.0
k_{-4}	4.47 E15	32.6
k_5	3.65 E15	31.3
k_{-5}	4.56* E14	31.3*

Davis plotted the ratio of the concentrations of HEIA to HEEDA and of TriHEIA to Trimer at various temperatures, versus the loss of MEA. From the results, the ratio of HEIA to HEEDA and of TriHEIA to Trimer were seen to track each other, suggesting similar equilibrium constants for the two pairs. The experimental data did not have enough TriHEIA in solution for the reverse reaction to be significant in the regression analysis. Subsequently, Davis assumed the pre-exponential factor to be $4{,}56 \cdot 10^{14}$ and the activation energy to be 31,3kcal/mol, which are the values denoted by a star in Table 3.3.1.

To summarize, Davis [5] solved the ODEs in Equation 3.2.2-3.2.8 by numerical integration, and by using the parameters in Table 3.3.1 to express the rate constants. These parameters were reported to minimize the sum of squared differences between the experimental and modeled values. The resulting model describes the concentration of MEA and the main degradation products as a function of time, initial amine concentration, CO_2 loading, and temperature.

Chapter 4

Model Evaluation

In modeling of chemical experiments, it is essential to evaluate of how close the model predictions are to the experimental data. General error equations are therefore used to quantify the accuracy of the models included in this thesis. The applied equations are presented in the following sections.

4.1 Absolute Error

The absolute error represents the absolute deviation between the modeled and experimental concentrations. The absolute error was calculated for all of the experimental points by utilizing Equation 4.1.1.

$$E_{abs} = C_{mod} - C_{exp} \tag{4.1.1}$$

Where C_{mod} defines the modeled concentration in mol/L at a specific time, aimed to describe the corresponding experimental concentration, C_{exp}.

According to Equation 4.1.1, model over-prediction is reflected by positive absolute errors, while negative absolute errors confirm model under-estimation of the experimental concentrations. The absolute error does not take into account the size of the measurements and is expected to increase by the value of the measurements. Therefore, the value of the absolute errors can be misleading when comparing absolute errors for measurements of varying sizes. It is then advantageous to include the relative errors.

4.2 Relative Error

The relative error conveys the magnitude of the absolute error, considering the size of the actual measurement. The relative error was calculated for all experimental concentrations by using Equation 4.2.1.

$$E_{rel} = \frac{C_{mod} - C_{exp}}{C_{exp}} \tag{4.2.1}$$

As opposed to the absolute error, the relative error takes into account the size of the measurement. Essentially, the magnitude of the relative error stays the same as the size of the measurement is varied and will not be affected by persistent experimental differences.

4.3 Average Errors

The average of the absolute and relative errors was calculated for different sets of concentration approximations. The term expressing the average error for a set of targeted experimental points is given by Equation 4.3.1.

$$E_{av} = \frac{\sum E}{m} \tag{4.3.1}$$

Where E represents the error, and m is the number of experimental points included in calculating the average.

In calculating the average absolute and relative errors, the positive and negative errors offset each other. Hence, the result of the average errors reveals a majority of over-or underestimation of data. In order to calculate the average deviation without regard to the sign of the errors, the average absolute values of the relative and absolute errors were calculated by 4.3.2.

$$E_{av} = \frac{\sum |E|}{m} \tag{4.3.2}$$

4.4 Root Mean Squared Error

The root mean squared error (RMSE) measures the standard deviation of the prediction errors in a model and is frequently employed to express the average performance error in model evaluation studies [25]. It is found by taking the square

root of the division of the sum of squares of the residual errors into the degrees of freedom, as given in Equation 4.4.1.

$$RMSE = \sqrt{\frac{\sum_{i=1}^{n} E_{abs}^2}{n-p}} \tag{4.4.1}$$

Where n is the number of data points used in the computation of the RMSE and p is the number of parameters in the model.

An RMSE value of zero would indicate a perfect fit for the data. Values close to the actual measurements indicate that the predicted values differ substantially from the experimental responses. In terms of model evaluation, the RMSE was mainly used to compare the accuracy of the different models. The RMSE was also used in the parameter fitting routine and will be further discussed in Section 6.3.

Chapter 5

Recreating Davis' Model and Extending the Data Set

5.1 Recreation of the Model

The first step in the model development was to regenerate the model by Davis, which was described in Chapter 3. Davis' model will be referred to as the original model.

The kinetic model from the original model, given in Equation 3.2.2-3.2.8, was implemented in Matlab. The temperature dependency of the rate constants was described by the Arrhenius equation, with the pre-exponential constants and activation energies found by Davis, listed in Table 3.3.1. The built-in solver in Matlab, *ode*45, solves nonstiff differential equations and was implemented to solve the system of model equations.

Comparison of the concentration profiles from the recreated and the original model required evaluation towards the same experimental basis. The experimental data used in the original model were available for MEA, HEIA, HEEDA, and Trimer. The corresponding data for TriHEIA was, on the other hand, not included in the report by Davis. However, some experimental points for TriHEIA were plotted in the graphs presenting the modeled and experimental values of MEA and the degradation products. The plots were associated with the full temperature range but limited to the experiments performed at loading 0.4. All integrated data describing TriHEIA were obtained from the plots, and the applied values are listed in Table D.0.1 in Appendix D. As a consequence of the limited experimental basis of TriHEIA, the recreated model could only be evaluated for TriHEIA at loading 0.4.

The concentration profiles from the recreated model were plotted for the different temperatures and CO_2 loadings, together with the corresponding experimental data. Additionally, the recreated model was evaluated utilizing the procedure in Chapter 4. The results are given in Chapter 7.

5.2 Extending the Data Set

The kinetic model and model parameters from the original model are solely based on the experiments by Davis. In order to better assess the performance of the model, degradation experiments from other researchers were included in the model. The added data enlarged the number of estimated data points and expanded the ranges of temperatures and CO_2 loadings described by the model. This way, the expanded data set enabled a more thorough evaluation of the model.

The experiments described in the *Literature Review*, in section 2.5, all provide experimental data that was used to extend the data set. Table 5.2.1 collects essential information for all included experiments.

Table 5.2.1: A summary of the number of applied data points from each researcher, the temperatures, CO_2 loadings and time ranges covered in the experiments, as well as the units of the data and a listing of the main degradation products.

REFERENCE	Data Points	T [°C]	CO_2 [mol CO_2/mol MEA]	Duration [Weeks]	Concentration Unit	Degradation Products
Davis [5]	104	100-150	0.2-0.5	16	mol/L	HEIA, HEEDA,TriHEIA, Trimer
Davis & Rochelle [14]	55	100-150	0.2-0.5	8	mol/kg H_2O	HEIA, HEEDA
Eide-Haugmo [21]	18	135	0.1-0.5	5	mol/L	HEIA, HEEDA, AEHEIA
Lepaumier et al. [4]	18	135	0.5	5	% of MEA loss	HEIA, HEEDA, AEHEIA
Léonard et al. [6]	22	120-140	0.4	3	mol/100g	HEIA, HEEDA
Zoannou et al. [22]	9	160	0.4	8	% of initial Nitrogen	HEIA, HEEDA
Fytianos et al. [23]	6	120	0.4	2	mol/L	HEIA, HEEDA
Fytianos et al. [26]	6	135	0.4	5	mol/L	HEIA, HEEDA

Common for all data given per volume or mass is that the associated reports omit information on whether the concentrations are given per loaded or per unloaded volume/mass. However, the most common procedure for the analytical methods is to subtract a fraction of the solutions for direct analysis. It was, therefore, assumed that the loadings were included in the volume/mass.

The already implemented data by Davis, and the majority of the experimental data in Table 5.2.1, are given in mol/L. Consequently, mol/L was the obvious choice of unit for the data set. All data given by other units was therefore converted to mol/L by the calculations shown in Appendix B.

All references use 30wt% MEA solutions, which refers to 300g MEA per kg water. Eide-Haugmo [21] and Leonard et al. [6] are the only researchers that include the actual measurement of the initial concentrations of MEA after the addition of CO_2. For all other researchers, the initial MEA concentrations were calculated at the reported CO_2 loadings and added to the experimental data. The approach of the calculations is shown in Appendix A.

The data listed in Table 5.2.1 was added to the model. No additional changes were made in the model, and the model was still defined by Davis' parameters. A new model evaluation was then performed to reveal the ability of the model to describe the newly added experiments. The results are presented in chapter 7.

Chapter 6

The final model

Davis found the optimal parameters to describe the results from his own experiments. New parameter values were found to give the best fit to the complete data set. A parameter fitting routine was therefore added to the code. Additional modifications were performed, and the details of the code development are described in the following sections.

6.1 Program Structure

An overview of the program structure of the final model is given in Figure 6.1.1.

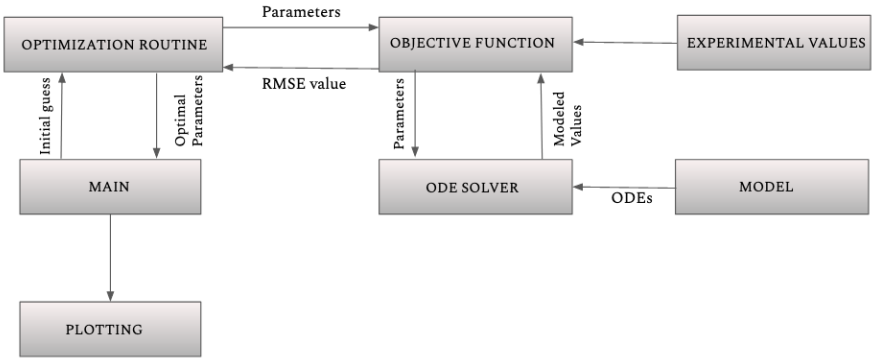

Figure 6.1.1: Flowsheet representing the structure of the code.

The main file includes specifications for the parameter fitting routine, depending on the chosen method. Both *fminsearch* and *particleswarm* were used as optimization tools, further explained in section 6.4. The parameter fitting routine uses the main file's specifications to send a set of parameters to the objective function.

The objective function forwards the suggested parameters to the ODE function file, which contain the ODE solver, $ode23s$, explained in Appendix E. The ODE file acquires the targeted ODEs from the model file and solves the system of differential equations by applying the suggested parameters. Consequently, the ODE file provides the solutions matrix that describes the modeled concentration profiles of the degradation compounds.

The object function receives both the concentration profile and experimental values and calculates the mean squared differences between the experimental and corresponding modeled values. The result is sent back to the parameter searching routine, and new parameters are found to lower the current error. The same procedure is repeated until the iteration tolerance is met.

As the minimum error is found, the main file calls the plotting file, which visualizes the results. The complete Matlab code is included in Appendix G.

6.2 The Model

In the model by Davis, the temperature dependence of the rate constants was described by the standard Arrhenius equation, given in Equation 3.3.1. The value of the pre-exponential factor, A, varies by an extensive value range, making it difficult to allocate a reasonable initial guess to this parameter. Additionally, the large range of values perplexes the search for the optimal parameter value. By reformulating the Arrhenius equation, the temperature dependency of the rate constant can be expressed by a reference rate constant, which is more intuitive to guess and lies within a smaller range. The result of the reformulation is equivalent to the original formulation but was used for simplicity and speed. The applied version of the rate constant is given in Equation 6.2.1.

$$k_i = k_{ref,i} \exp(-\frac{E_{a,i}}{R} \frac{1}{T_i} - \frac{1}{T_{ref}}) \tag{6.2.1}$$

Where k_{ref} is the reference rate constant and T_{ref} is the reference temperature, set to 400K.

The parameters to be optimized in the final model were the reference rate constants, k_{ref}, and the activation energies, E_a. Instead of optimizing the reference rate constants and activation energies directly, the parameters were defined as ten to the power of an exponent, as shown in Equation 6.2.2.

$$k_{ref,i} = 10^{x_i} \qquad E_{a,i} = 10^{x_i} \tag{6.2.2}$$

The parameter fitting routine was targeted to find the optimal exponents. By this definition, the parameter estimates are assured to be of the same order of magnitude, which simplifies and quickens the optimization. Another advantage is that the activation energies and reference rate constants are assured positive, independent of the choice and definition of the solver. In general, the transition state of a reaction is at a higher level of energy than the reactants or products, which entails positive activation energies. Additionally, the rate constants have already been defined as the forward or reversed reactions in the kinetic model, suggesting positive reference rate constants.

6.3 Choosing the Error Function

As briefly mentioned in Chapter 4, the RMSE was chosen as the objective function. A common concern related to this error term is its sensitivity to outliers. The residual errors are squared before averaged, which means that significant errors are given relatively large weights. In thermal degradation, the largest prediction errors are expected to be designated MEA, due to relatively high concentrations. MEA will, therefore, contribute the most to the total RMSE and be weighted the most when minimizing the total model error. As previously explained, the loss of MEA induces perceptible costs to the PCC system, and the concentration of the MEA is therefore considered the most critical to predict. For this reason, the sensitivity of the RMSE to outlier is used to prioritize the prediction of MEA. By using the RMSE as the objective function, the parameter fitting emphasizes the most prominent compounds rather than those of small concentrations.

6.4 Methods of Parameter Fitting

The optimal reference rate constant and activation energies were found to minimize the objective function. Two different parameter routines were utilized in the progress of optimization, and the methods are described in the following sections.

6.4.1 Simplex Iteration

The built-in Matlab solver *fminsearch* finds the minimum of unconstrained multivariable functions, by simplex iteration. It uses the following syntax.

x = fminsearch(fun,x0)

The *fminsearch* algorithm uses a simplex of n+1 points for n-dimensional vectors x. It starts by making a simplex around the initial guess, x0, by adding 5% of each parameter value corresponding to x0. For each iteration, the n vectors as elements of the simplex and the current point are evaluated. The algorithm modifies the simplex repeatedly to obtain the lowest function value. The iterations continue until the stopping criterion is reached. The solution, x, is then returned as a real array or vector of the current parameter values.

fminsearch is a reasonably fast and straightforward parameter fitting method. However, the disadvantage of this method is that the solver locates the nearest minimum from the initial guess and does not distinguish between local or global minimums. Hence, finding the global minimum depends substantially on the initial guess. Numerous different local minimums were found when adjusting the initial guesses in the model. It was therefore concluded that the objective function possesses too many local minimums for *fminsearch* to be efficient.

6.4.2 Particle Swarm Optimization

Particle Swarm is a population-based algorithm aimed at optimizing nonlinear functions. The syntax of the particle swarm solver is given below.

x = particleswarm(fun,nvars,lb,ub)

Where *fun* is the function to be minimized and *nvars* is the dimension of *fun*. A certain amount of particles are spread out in a specified region, which is limited to the lower boundary, *lb*, and the upper boundary, *ub*, of each parameter. The particles are assigned initial particles, and each represents different values of the objective function with specific combinations of parameter values. For each new location, the particles choose new velocities based on the current velocity, the particles' individual best locations, and the best locations of their neighbors. This way, the particles cooperate to find the minimum. The iterations proceed until the algorithm reaches a stopping criterion. At this stage, the particles have coalesced around one or more locations, depending on the presence of local minimums. The best value found by any of the particles in the swarm is tracked, representing the global minimum within the specified region. The corresponding parameter values are returned as a vector or matrix, x.

This method is more time-consuming than simplex iteration, as it searches through a whole area and requires a large number of iterations. However, the method is more reliable as it is not dependent on the initial guess. Still, the method requires specified parameter intervals that contain the values corresponding to the optimal solution. Due to the large number of local minimums in the objective function, particle swarm optimization was considered the most suitable to find the global minimum for the final model.

6.5 Challenges during Optimization

Both parameter fitting methods adjust the values of the reference rate constants and the activation energies within specific ranges in the search for function minimums. When the parameter fitting routine combines reference rate constants and activation energies that both amplify the reaction rate, the value for the reaction rate becomes unrealistically high, which causes difficulties for the ODE solver. In this work, a manual value of the objective function was set each time this problem emerged. The value was assured higher than what was obtained when the result converged.

6.6 Adding AEHEIA data

As explained in Section 2.4.2, the lack of standards complicates the determination of the exact structures of some of the degradation products. In the degradation pathways described by Davis [5], Lepaumier et al. [4], and Eide-Haugmo et al. [21], TriHEIA and AEHEIA are formed at the same stage in the pathway and by the same reactants. TriHEIA and AEHEIA are very similar in mass and polarity, making them difficult to distinguish without standards for the retention time. Therefore, it was hypothesized that Davis and Lepaumier/Eide-Haugmo report the same product but have concluded with slightly different structures. For this reason, the measurements of AEHEIA from Lepaumier and Eide-Haugmo were added to the final model, and compared to the model description of TriHEIA. The results are given in Section 9.5.

Part III

Results and Discussion

Chapter 7

Recreation of Davis' Model

The model by Davis [5] was recreated by the procedure described in Chapter 3 and the model gave a total RMSE of 0.0805 mol/L. Considering the size of the measurements of MEA, which ranged from around 4.9 to 1.87 mol/L, the average magnitude of the residuals is relatively low. The RMSE, therefore, indicates a good fit for the model predictions of MEA. It is more difficult to manifest the fit to the components of less extensive concentrations based on the value of the RMSE. The average errors of all components were therefore calculated and tabulated in Table 9.2.1, presented in Chapter 9. The results revealed relatively good model descriptions of HEEDA, HEIA, and Trimer, with average relative errors of around 10%. The predictions of TriHEIA were less precise, with an average relative error of 24%.

The experiments included in Davis' model were plotted towards the corresponding prediction given by the recreated model. Figure 7.0.1 illustrates the result from plotting one of the experiments.

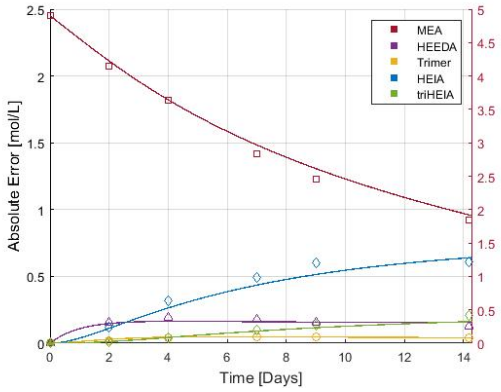

Figure 7.0.1: Example of plotting one of Davis' [5] experiments by using the recreated model. The lines represent the modeled concentrations, and the points represent the experimental concentrations at 393K and initial CO_2 loading of 0.4. The right axis is scaled for MEA, and the left axis is scaled for the degradation products.

The report by Davis includes plots that illustrate the predictions of the experimental points for all temperatures at an initial CO_2 loading of 0.4. Comparison between the obtained results from the recreated model, including Figure 7.0.1, with the results given by Davis verified an apparent similarity between the original and recreated model.

Along with the plots, Davis reported the average relative error for a set of selected experimental and modeled values for MEA, HEEDA, and HEIA. The corresponding errors were found for the recreated model to assure its accordance with the original model. Table 7.0.1 compares the average of the selected relative errors in the original model with the corresponding errors in the recreated model.

Table 7.0.1: The average relative errors reported by Davis and the corresponding average relative errors calculated for the recreated model.

Model	**MEA**	**HEEDA**	**HEIA**
Davis	0,059	0,12	0,18
Recreated	0,055	0,13	0,20

Table 7.0.1 reveals proximity between the average relative errors found for MEA, HEEDA, and HEIA in the recreated and the original model. Hence, the comparison of the model errors indicates a successful recreation of the model for the respective components. The lack of reported errors for triHEIA and Trimer makes it difficult to compare the prediction of these components in the two models. For this reason, it can not be stated by certainty that Davis' model was fully recreated. However,

visual comparison of the plots from the experiments at loading 0.4 discloses a similar representation of TriHEIA and Trimer as well. So, based on matching degradation plots and similar average errors for MEA, HEIA, and HEEDA, Davis' model is concluded to be successfully recreated.

Chapter 8

Extending the data set

Experimental data for MEA, HEEDA, and HEIA were added to the model, as described in Section 5.2. The ability of the model to describe the additional experiments was examined by comparing the model precision before and after supplementing data. After the inclusion of data, the RMSE was calculated to 0.2283 mol/L, which is close to a tripling of the previous RMSE. For most concentrations of MEA, the average deviation constitutes a relatively low share of the measured concentrations. However, for the lowest MEA concentrations, typically found at high temperatures and CO_2 loadings, the average RMSE indicates significant deviations. The average residuals are even more significant compared to the measurements of HEEDA and HEIA, suggesting notable prediction errors for the two degradation products.

To further investigate the reduced overall model performance, the errors were investigated for each component. Figure 8.0.1 illustrates the change of absolute and relative errors for each component before and after the addition of data.

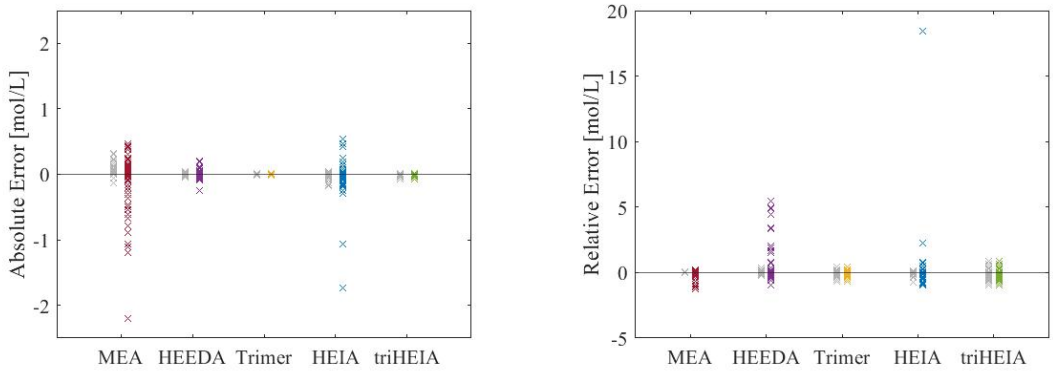

(a) Absolute Errors

(b) Relative Errors

Figure 8.0.1: Absolute and relative errors for all experimental points included in the recreated model, before and after inclusion of more data. The errors in the model describing only Davis' experiments are marked in grey, and the errors for the complete data set are colored.

It is clear from Figure 8.0.1, that the average errors have increased for MEA, HEEDA, and HEIA by the addition of data. In order to concretize the visualized errors, the average of the errors and the average absolute valued errors were calculated for the different components and tabulated in Table F.0.1, in Appendix F, and in Table 9.2.1. Most prominent is the high relative errors of HEIA and HEEDA in Table 9.2.1, and the vast majority of MEA underestimation established from Table F.0.1. The underprediction of MEA was not delimited to experiments performed by certain researchers or at specific experimental conditions. However, the most substantial relative errors were connected to the experiments by Zoannou.

Figure 8.0.2 illustrates the model predictions of one of the experiments by Zoannou, and is selected to illustrate the high relative errors of HEIA and HEEDA, and to represent the general trend of underprediction of MEA.

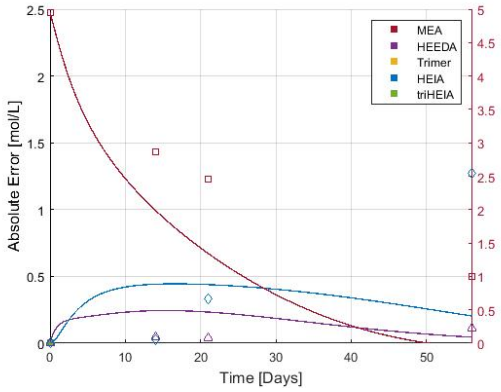

Figure 8.0.2: A selected plot that illustrates the underestimation of MEA and high relative errors for HEIA and HEEDA after including additional data to the recreated model. The experiment was performed by Zoannou at 160°C and loading 0.19.

Calculations of the absolute and relative errors in Figure 8.0.1 established increased absolute and relative errors for MEA, HEEDA, and HEIA, of which new data was included. The results from the calculations are included in Table 9.2.1, which is presented in the next chapter. The increased errors caused by the addition of data demonstrate that Davis' model is not as precise at predicting the experiments by other researchers as to describe the experiments performed by himself. Therefore, the conclusion of optimizing the parameters was made to obtain the best fit for the whole data set.

Chapter 9

The final model

9.1 Optimized Parameters

The temperature-dependent rate constants were found by using the modified Arrhenius equation, given by Equation 6.2.1. The optimal parameter values for the complete data set were found as described in section 6, and listed in Table 9.1.1.

Table 9.1.1: Optimized values for the reference rate constants, K_{ref}, and the activation energies, E_a, used in the final model.

Rate constant	$\mathbf{k}_{ref}$ **[L day^{-1} mol^{-1}]**	$\mathbf{E}_a$ **[J/mol]**
k_1	1.51937 E-3	1.32081 E5
k_2	1.25044 E-1	4.2130 E4
k_3	2.67772 E-1	7.51734 E4
k_4	1.72871 E-1	3.5627 E4
k_{-4}	5.17217 E-5	2.90907 E4
k_5	2.10748 E-3	3.82210 E5
k_{-5}	3.97067 E-2	1.09901 E4

When recreating already existing models, a common challenge is that the reported parameters do not match the reported results. Consequently, it is not possible to recreate the model by using the reported parameters. When operating with parameters multiplied by 10^5, the number of decimals may be of great importance to the final result. To prevent inconsistency between the parameters and the presented results, the parameters exactly as given in Table 9.1.1 were used to calculate and the RMSE and generate the plots.

9.1.1 Comparison to Literature

As mentioned in Section 2.5, Leonard et al.[6] developed a rate expression for the loss of MEA, based on the experimental results at 140 and 120°C and at loading 0.44. The given rate expression enabled comparison of the initial rate of MEA given by Leonard et al.[6], to the initial rates found for Davis' model and the final model, given by Equation 3.2.2. Table 9.1.3 compares the initial rates of MEA loss given by Leonard, to the initial rates calculated for Davis' model and for the final model.

Table 9.1.2: Initial rates of MEA loss at 120 and 140°C found for Leonard[6], Davis[5] and for the final model, given in [molL^{-1}day^{-1}].

Reference	**120**°C	**140**°C
Leonard	0.0101	0.0858
Davis	0.0164	0.1386
Final Model	0.0158	0.1122

Table 9.1.3 reveals similar initial rates for the three models, suggesting similar initial slopes for MEA at the given temperatures. Leonard's model provides a slightly lower rate and therefore indicates less initial degradation of MEA than seen for the other two models. Accordingly, Davis' model and the final model were observed to slightly underestimate the experimental data of MEA used in the model by Leonard at the given temperatures. Furthermore, Table 9.1.3 states that the initial rate of MEA loss is slightly higher for Davis' model than for the final model at 120 and 140°C.

The activation energies found by using the final model, in Table 3.3.1 were converted into kcal/mol and compared to the ones listed by Davis.

Table 9.1.3: The activation energies found in this work, compared to the activation energies found by Davis.

Activation Energy	**This Work [kcal/mol]**	**Davis' Model [kcal/mol]**
E_a1	31.6	34.4
E_a2	10.1	33.3
E_a3	18.0	31.5
E_a4	8.52	33.0
E_a-4	6.95	32.6
E_a5	91.4	31.3
E_a-5	2.63	31.3

As seen in Table 9.1.3, Davis found similar activation energies for all reactions, whereas the corresponding activation energies found in this work varies distinctly. The similar values found by Davis suggest that the mix of products will not be a function of temperature. The same conclusion can not be made based on the activation energies found in this work.

9.2 Model Evaluation

The parameters found by Davis were replaced by the optimized values in Table 9.1.1, to give a better fit to the complete set of experimental data. The resulting RMSE of the final model was found to be 0.1536, reflecting a reduction of 30% from the model with Davis' parameters. The overall improvement by using the optimized parameters, rather than Davis' parameters, is elaborated by investigating error plots and calculations.

Figure 9.2.1 compares the absolute and relative errors for the final model and the model using Davis' parameters.

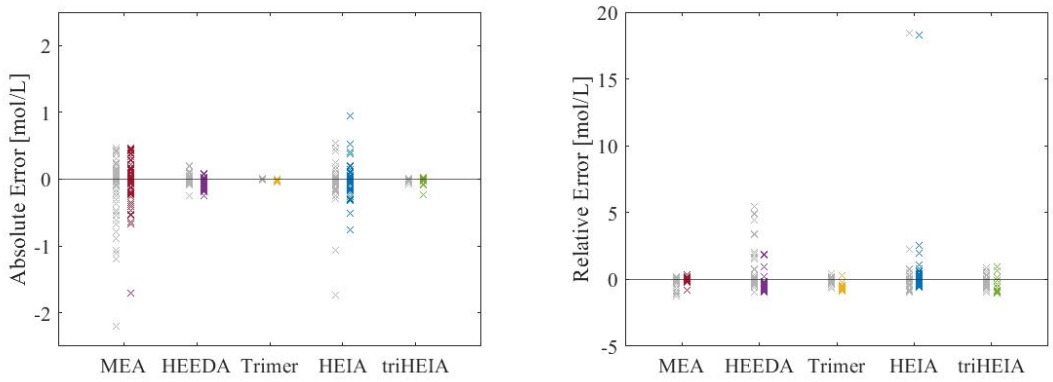

(a) Absolute Errors

(b) Relative Errors

Figure 9.2.1: Absolute and relative errors for all experimental points included in the model using Davis' constants and the model using the optimized model. The results from using the parameters by Davis with the complete data set is marked in grey, and the result when using the optimized parameters is marked in colors.

The average of the absolute and relative errors included in Figure 9.2.1 was calculated for each component and included in Table 9.2.1.

Table 9.2.1: Average of the absolute deviation for all the experimental points used in each model.

		MEA	HEEDA	Trimer	HEIA	TriHEIA
Data and parameters by Davis	**Abs Err**	0.0773	0.0099	0.0033	0.0263	0.0076
	Rel Err	0.0215	0.0787	0.1198	0.0993	0.2390
All data with Davis' parameters	**Abs Err**	0.1822	0.0613	0.0033	0.0938	0.0076
	Rel Err	0.0858	0.8763	0.1198	0.7685	0.2390
All data with optimal parameters	**Abs Err**	0.1510	0.0559	0.0157	0.0932	0.0279
	Rel Err	0.0533	0.7545	0.6977	0.7678	0.7764

All error plots and calculations of the average errors include the first point in the predictions. The ODE solver integrates from the initial concentration given by the experiments, which means that the first point will not contribute to prediction error. Inclusion of the initial concentration adjusts the calculated average errors towards zero and slightly embellishes the presented model errors. In this thesis, the average error calculations are mainly used to compare the models and the accuracy for each component, so the affection of the initial points has no practical significance.

9.2.1 MEA

From Figure 9.2.1a, the absolute errors for MEA appears large. However, the quantities of MEA are relatively large, which results in the small relative errors seen in Figure 9.2.1b. Table 9.2.1 establish a reduction in the average errors in the MEA predictions when using the optimized parameters, compared to Davis' parameters. The prediction deviates by about 5%, which means that the model generally provides a good prediction of MEA. Figure 9.2.1 shows that there is no clear trend of model over- or underprediction in the fitting of MEA.

By comparison of the average relative errors in Table 9.2.1, the model prediction fits better for MEA than for the other components. This observation is in accordance with the choice of RMSE as the object function, as discussed in Section 6.3. Essentially, the relatively large contribution of MEA to the object function causes the fitting of MEA to be emphasized to a larger degree than the remaining components during the

parameter fitting. Additionally, there is considerably more experimental data available for MEA than for the remaining components. The relatively high number of data points amplifies the contribution from the MEA measurements to the RMSE and the corresponding strive to fit the experimental values of MEA.

9.2.2 HEIA

Table 9.2.1 reveals a slight improvement in the accuracy of the modeled HEIA concentrations by using the optimized parameters. Figure 9.2.1 illustrates that the improvement is not significant, and there are still some clear outliers in the plots. No prominent trend of under-or overprediction of HEIA is seen in Figure 9.2.1.

HEIA is the degradation compound of the most considerable quantity, and the corresponding prediction errors contributes second most to the RMSE before the optimization, as seen in Table 9.2.1. Due to the relatively significant error contribution, the slight improvement by optimization was somewhat unexpected. However, in addition to the priority of fitting MEA during the parameter fitting, the optimization routine emphasizes the fit of the actual outliers. For some cases, it might give a more considerable reduction of the total error by adjusting the prediction towards the extreme points than to fit the relatively small error contributions from the more realistic points. This tendency is a constrain to the chosen objective function. The improvement of the outliers, seen in Figure 9.2.1, can therefore be at the expense of improving the fit to the remaining experimental points. The outliers are essentially results of deviations in the experimental data. Such variations are believed to be a part of the explanation to the small improvement seen for HEIA.

Essentially, the optimization could not reduce the average error associated with HEIA to a significant degree, despite the relatively large error contribution caused by the predictions of HEIA. As a result, the estimations of HEIA contribute considerably to the final value of the RMSE.

9.2.3 HEEDA

Table 9.2.1 discloses a modest improvement of the HEEDA predictions by optimization. As seen in Figure 9.2.1, the largest relative errors have been reduced, but the model now underestimates the majority of the experimental points.

The same number of experimental points were used for HEEDA as for HEIA, but HEEDA is measured in smaller quantities. It would therefore be expected that the improvement of HEIA was larger than for HEEDA. This was, however, not the case, as HEEDA was more significantly improved, as seen in Table 9.2.1. Still, there are significant deviations between the predicted and experimental values of HEEDA, as presented in Figure 9.2.1. These deviations are considered partly due to experimental differences but mainly due to the parameter fitting, as the error contribution from HEEDA is relatively small compared to MEA.

9.2.4 Trimer and TriHEIA

As opposed to the other components, Table 9.2.1 shows a decreased model accuracy for the estimations of Trimer and TriHEIA in the final model. Figure 9.2.1 discloses a clear trend of underestimation of both TriHEIA and Trimer.

Trimer and TriHEIA are reported to be the components of the smallest concentrations, and the related average errors are therefore the smallest. For this reason, the associated error contributions are of little significance to the total RMSE. This, in addition to the relatively few data points, explains why the predictions of these components are worsened on behalf of the improvements seen for the other components.

9.3 Illustrations of the prominent trends

Figure 9.3.1 shows the modeled predictions for a selection of experiments.

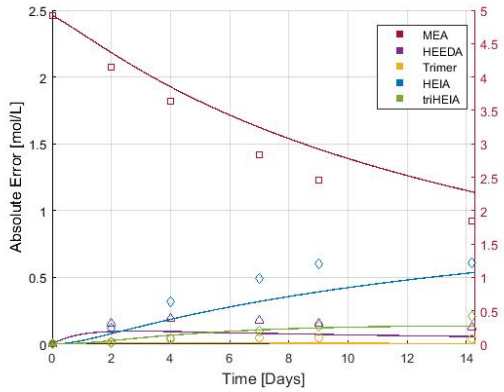

(a) Experiment by Davis [5] at 423K and CO_2 loading 0.4.

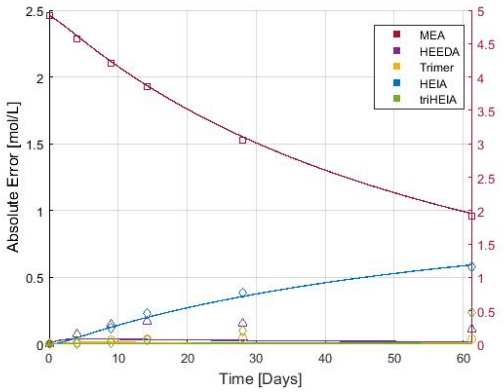

(b) Experiment by Davis [5] at 408K and CO_2 loading 0.4.

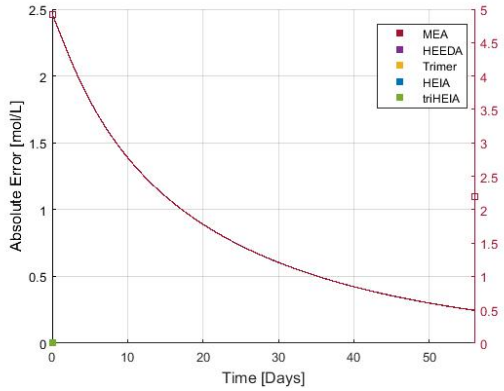

(c) Experiment by Davis and Rochelle [14] at 423K and loading 0.4.

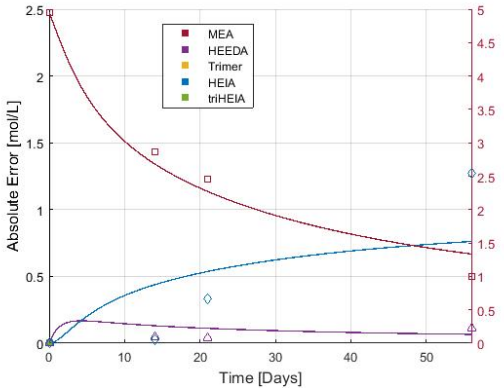

(d) Experiment by Zoannou et al. [22] at 433K and loading 0.19.

Figure 9.3.1: A selection of model predicted experiments.

Figure 9.3.1a, 9.3.1b and 9.3.1d all present the overall precise fittings to MEA, which resulted in low relative errors for MEA. The exception is seen in Figure 9.3.1d, where the predicted value of MEA deviates substantially from the experimental value. This point appears as a clear outlier in Figure 9.2.1a.

The general trends of underestimating HEEDA, Trimer and TriHEIA are illustrated in Figure 9.3.1a and 9.3.1b. Significant relative deviations are linked to the respective predictions in the two figures. The largest relative error was seen for HEIA, and the clear outlier in the plot of the relative errors in Figure 9.2.1b is caused by the prediction in Figure 9.3.1d. Figure 9.3.1a, 9.3.1b and 9.3.1d illustrate that there is no clear trend of over -or underprediction of HEIA.

9.4 Experimental Basis

The model aims to find the dependency of degradation on temperature and CO_2 loading, based on the experimental data. The value of the modeled results is therefore highly dependent on reliable experimental data. Suppose the experimental measurements between the researchers vary. It is then difficult to fit the different experiments by the same kinetic model and to provide a representative and realistic dependency of the temperature and loading.

The majority of the applied researchers report having investigated 30wt% MEA for given CO_2 loadings by the procedure described in Section 2.4.1. However, the experimental data is seen to deviate at identical conditions between researchers. For instance, the degradation in the experiment by Lepaumier gave 14% more degradation than Eide-Haugmo, and the measured concentration of HEIA reported by Lepaumier after five weeks was higher than the corresponding measurement reported by Davis and Rochelle [14] after eight weeks. There is no obvious explanation for the deviations between the reported data, and it is not clear if the differences are caused by the applied analytical methods or experimental factors. However, the level of detail included in the information available from the publications varies a lot. For instance, some researchers have checked for leakages in the system and have assured the correct initial loading and amine concentration, while others omit such information in the reports. The inconsistency in the included experimental information cause uncertainty in the experimental basis of the results and the comparability of the data by the different researchers.

As already presented, Figure 9.3.1c is the source to the largest absolute error for MEA, and the designated point is linked to the experiment by Davis [5] at 150°C. All other experiments by Davis [5] were described precisely by the model. The other experiments performed by Davis and Rochelle [14], at 150°C, were also satisfactorily described. It is, therefore, difficult to explain the large average deviation seen for this exact experiment. Essentially, the considerable degradation in the experiment does not follow the same temperature dependency as the other experiments and could not be fitted as well as the others.

The largest errors for HEIA and HEEDA were found in the predictions of the two experiments by Zoannou [22]. The result from plotting the experiment by Zoannou with CO_2 loading 0.19 is illustrated by Figure 9.3.1d, and the experiment at loading 0.39 showed a similar result. The loss of MEA is well described for both experiments, but the predictions of HEEDA and HEIA are observed to deviate significantly from the experimental values. These deviations appear as outliers in Figure 9.2.1. The significant difference between the precision errors for Zoannou's experiments and the rest of the experiment is hypothesized to be expounded by the different experimental setup. As mentioned in Section 2.5, the experiments by Zoannou were performed in an open design, while the other experiments were performed in closed systems. This may have caused the large errors linked to the experiments by Zoannou. However, there is no obvious explanation as to why the different setup could cause the distinctive result.

9.4.1 Dependency of Experimental Conditions on Model Performance

The absolute and relative errors associated to each of the components are plotted as a function of time, loading and temperature, encapsulated in Figure 9.4.1.

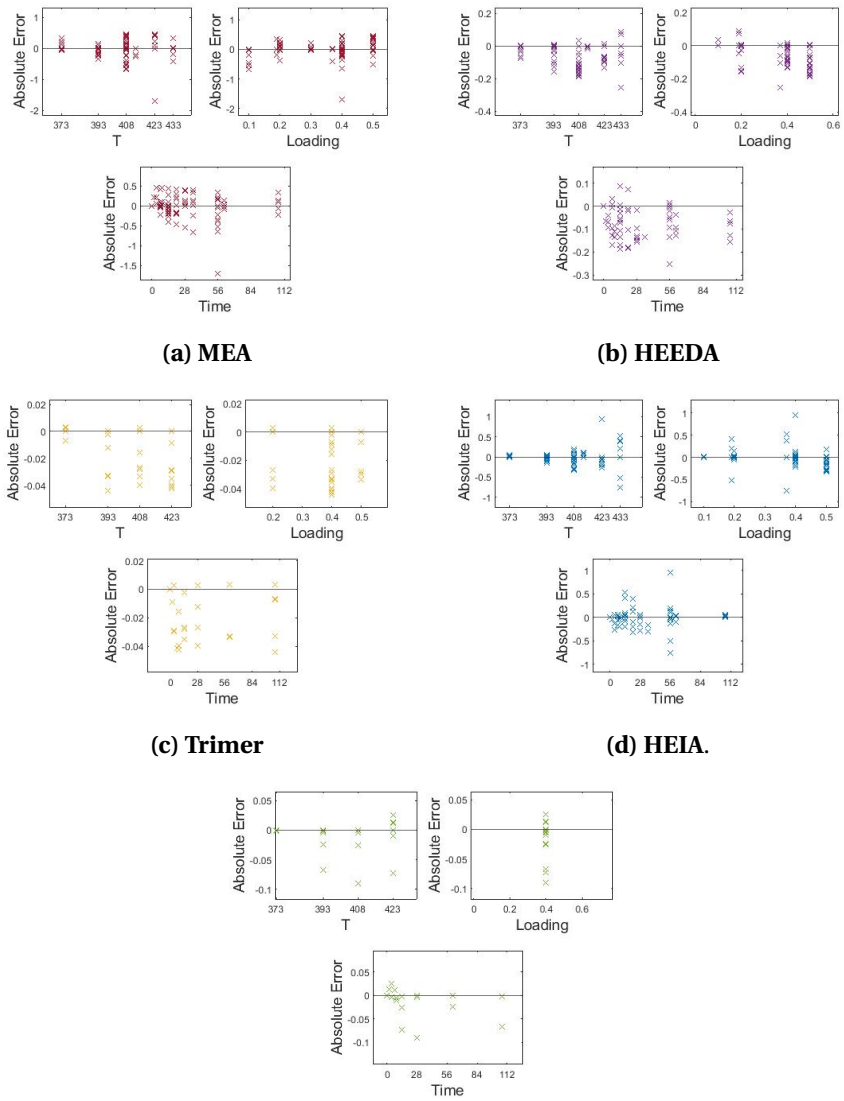

(a) MEA

(b) HEEDA

(c) Trimer

(d) HEIA.

(e) TriHEIA

Figure 9.4.1: The absolute errors [mol/L] plotted for MEA, HEEDA, Trimer, HEIA, and TriHEIA as a function of temperature [K], CO_2 loading[mol CO_2/mol MEA], and duration of the experiments [days].

Figure 9.4.1 shows that there is no clear correlation between the accuracy of the model prediction for the different degradation components and the temperature, CO_2 loading, or duration of the experiments.

9.5 Adding AEHEIA data

As explained in Section 9.5, the possibility of confusion of TriHEIA, identified by Davis, and AEHEIA, found by Eide-Haugmo and Lepaumier, was considered. Therefore, the experimental results for AEHEIA were included in the model to investigate its fit to the modeled TriHEIA. The results are plotted in Figure 9.5.1a and 9.5.1b.

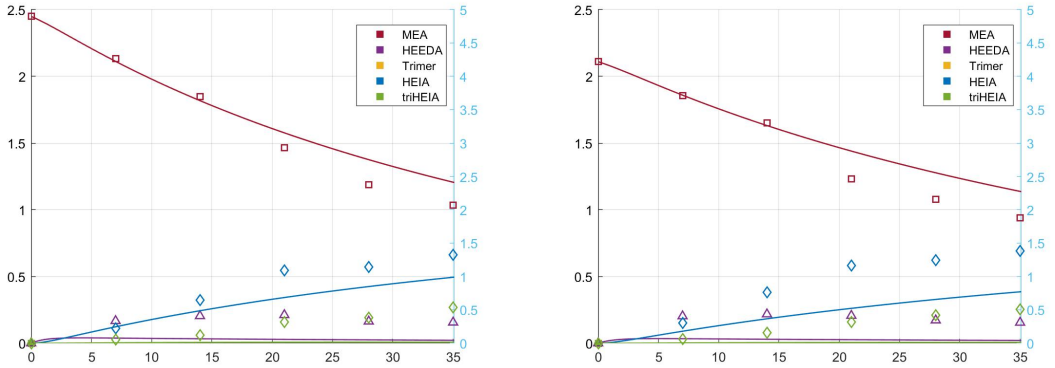

(a) Experiment by Lepaumier et al [4].

(b) Experiment by Eide-Haugmo [21].

Figure 9.5.1: Experiments by Lepaumier and Eide-Haugmo at 135°C and loading 0.4. The green points represent the experimental values of AEHEIA, and the green line represents the modeled prediction of TriHEIA.

The clear under-prediction of AEHEIA in 9.5.1a and 9.5.1b is consistent with the general underestimation of TriHEIA, which was seen in Figure 9.4.1. However, the predicted values of TriHEIA in the final model are not sufficient to describe the TriHEIA, and it is therefore difficult indicate whether AEHEIA could be described by the prediction of TriHEIA. A model that adequately represents TriHEIA would make it easier to indicate similarity between the model descriptions of TriHEIA and the experimental AEHEIA. No conclusions are therefore made, based on the result in 9.5.1, but the results are included to point out the possibility that TriHEIA and AEHEIA might be mixed up due to the lack of available standards.

9.6 Evaluation of the kinetic model

The activation energies listed in Table 9.1.3, showed a higher activation energy for HEIA than HEEDA, suggesting a higher stability of HEEDA in the equlibrium reaction. This is not in accordance with the experimental measurements, as HEIA is the main degradation product in all of the studied experiments. Additionally, the exceedingly high activation energy, Ea5, suggests high stability of Trimer and little formation of TriHEIA. Again, the experiments confirm the opposite, as the applied concentrations of TriHEIA are more extensive than of Trimer. Consequently, the associated activation energies do not seem realistic, and the ability of the kinetic model to represent thermal degradation experiments is therefore questioned.

According to a study performed by Tontiwachwuthikul and Idem [27], the formation of bicarbonate accelerates at higher CO_2 loadings. This formation is not included in the kinetic model by Davis [5], and the absorption of CO_2 in Davis' model is therefore based on the assumption that the absorption occurs solely by carbamate formation. Davis [5] used CO_2 as a surrogate for OZD, which participates in the majority of the involved reactions. By formation of bicarbonate, the concentration of OZD at higher loading is not proportional to the consumed CO_2 in the formation of carbamate. It was therefore hypothesized that the formed bicarbonate in the experiments at high loadings would lead to an overestimation of CO_2. This would accelerate the modeled carbamate polymerization and come across as model overestimation of the degradation products. However, the prediction errors for the model are not observed to be particularly large at high loadings compared to lower loadings. Additionally, most of the degradation products are, in fact, underpredicted by the model. So, based on the results, there is no reason to believe that the omission of bicarbonate from the kinetic model has impacted the modeled results.

Davis [5] identified MEA Urea and included it in the degradation pathway as a product from the reaction between MEA and OZD, given in Reaction RX3. However, MEA Urea was not included in the kinetic model. The inclusion of MEA Urea would cause more CO_2 to be consumed, leading to less formation of the consecutive degradation products and amplified underestimation of the measured products. Again, there is no indication from the modeled result that MEA Urea should be included in the kinetic model for improved results.

Part IV

Conclusions and Recommendations

Chapter 10

Conclusion

An already existing model was recreated, describing MEA, HEIA, HEEDA, Trimer, and TriHEIA as a function of temperature and CO_2 loading. The included data set was expanded to evaluate the model precision for experiments from different researchers at extended ranges of temperatures and CO_2 loadings. The inclusion of data describing MEA, HEIA, and HEEDA entailed increased average prediction errors for all three components. An optimization routine was therefore implemented to improve the fit to the full experimental data set. By applying the optimal parameters found by particle swarm optimization, the total root mean squared error (RMSE) was reduced by 30%. The best predictions were seen for MEA, given by the average relative error of 5%. The descriptions of the two most extensive degradation products, HEIA and HEEDA, were also slightly improved by the optimization to average relative errors of 77 and 75%. The corresponding prediction errors for TriHEIA and Trimer, were calculated to 78 and 70%, reflecting a significant increase by the implementation of the optimal parameters. As no additional data was included for these two components, the increased errors were purely on behalf of fitting the other components.

The advantage of using the RMSE as the objective function was the emphasized fitting of MEA, but a consecutive constrain the emphasis of outliers and downgrade of fitting degradation products, due to relatively small concentrations. Differing experimental data were found for HEIA and HEEDA, which was also considered a substantial source of high prediction errors. Finally, the activation energies found for the equilibrium reactions between HEIA/HEEDA and Trimer/TriHEIA favored the formation of HEEDA and Trimer, which is not in accordance with the experimental results. The unrealistic model parameters provided by the kinetic model arise doubt to the adequacy of the model. Insufficient model descriptions would be an essential source of deviations for the model.

Chapter 11

Further Work

The current model was shown to provide a reasonably good description of MEA but has a clear potential for improvement for the predictions of the degradation products. It is preferred to develop a model that can adequately represent all of the degradation compounds. It would therefore be interesting to investigate the impact on the predictions by changing the objective function. For instance, use of a weighting factor of the errors, as discussed by Cleger-Tamayo et al. [28], enables weighing of errors in the same magnitude for all components. This is likely to improve the fitting to the degradation products' results, but the estimation of MEA is likely to decrease. However, it would be interesting to see the extent of penalty to the errors for MEA induced by changing the objective function. For the case of a low penalty, other choices of the objective function might be preferred.

The activation energies were not found to be realistic, and it was argued that there is room for improvement of the kinetic model. It is difficult to state the exact changes that should be done to the kinetic model, but several approaches can be tested. For example, the dependency between the concentration of reactants and products might be introduced by the equilibrium constant instead of using separate forward and reverse reactions. It would also be possible to simplify the equilibrium reactions by only considering the forward reaction. Additionally, the inclusion of bicarbonate and MEA Urea might also be relevant to include in future models.

There are not many extensive experiments performed on thermal degradation and there is not a large quantity of experimental data included in the model. More data would give a better basis for model evaluation and improve the reliability of the provided results. By adding data, the total weight on the outliers would also decrease, which is likely to improve the results.

The possible confusion between TriHEIA and AEHEIA should be further considered. By confirmed mixup, the applicable data set of TriHEIA/AEHEIA would be expanded, which would give a better basis to evaluate the model precision for the established component.

Significant experimental deviations between experiments were encountered for some components at identical conditions. It is uncertain whether the differences are caused by the applied analytical methods or by experimental factors. Efforts should therefore be made to investigate the source of these deviations. To facilitate the investigation, future reports should include a high level of detail in the experimental procedures.

The current model is developed to fit degradation from 30% MEA solutions. By including data provided for solutions of varying initial amine concentrations, the consecutive impact on the model performance can be assessed. There might also be other factors affecting the occurring thermal degradation, such as acid or metal concentrations. The impact of such elements can be investigated and potentially included in the model.

By eventual achievement of an adequate model that is representative for the industrial plants, the model can be used to optimize the stripper conditions. By predicting the loss of MEA, the related costs can be calculated and evaluated towards the energy costs.

Bibliography

[1] Jeong Y.S Lee U. Lim Y. Yang S. Lee C.S. Kim J. Jung, J. and C. Han. Combustion co2 capture process with aqueous mea: An advanced mea process using a phase separation heat exchanger. *Computer Aided Chemical Engineering*, 31(8):505–509, 2012. doi: https://doi.org/10.1016/B978-0-444-59507-2.50093-7.

[2] Dillon C.P. Poldermann, L.D. and A.B. Steele. Why monoethanolamine solution breaks down in gas treating service. *Proc. Gas Conditioning Conf*, pages 49–56, 1955.

[3] Zelenskaya L. G. Yazvikova, N. V. and L. V. Balyasnikova. Mechanism of side reactions during removal of carbon dioxide from gases by treatment with monoethanolamine. *Zhurnal Prikladnoi Khimii*, 3(48):674–676, 1975.

[4] da Silva E. F. Einbu A. Grimstvedt A. Knudsen J. N. Zahlsen K. Lepaumier, H. and Svendsen H. F. Comparison of mea degradation in pilot-scale with lab-scale experiments. *Energy Procedia*, 4:1652–1659, 2011. doi: https://doi.org/10.1016/j.egypro.2011.02.037.

[5] J. D. Davis. Thermal degradation of aqueous amines used for carbon dioxide capture. *The University of Texas at Austin*, Doctor of Philosophy, 2009. doi: https://rochelle.che.utexas.edu/files/2015/02/Davis-2009-Thermal-Degradation-of-Aqueous-Amines-Used-for-Carbon-Dioxide-Capture.pdf.

[6] T. Léonard G., Toye and G. Heyen. Experimental study and kinetic model of monoethanolamineoxidative and thermal degradation for post-combustion co2capture. *International Journal of Greenhouse Gas Control*, 30:171–178, 2014. doi: https://doi.org/10.1016/j.ijggc.2014.09.014.

[7] NASA. Overview: Weather, global warming and climate change. https://climate.nasa.gov/resources/global-warming-vs-climate-change/s, . Reading date: 05.02.21.

[8] NASA. The causes of climate change. https://climate.nasa.gov/causes/, . Reading date: 05.02.21.

[9] D. Picq Lepaumier, H. and P. Carrette. New amines for co2capture. i. mechanisms of amine degradation in the presence of co2. *Industrial Engineering Chemistry Research*, 48:9061–9067, 2009. doi: https://doi.org/10.1021/ie900472x.

[10] A. Basile and P. Marrone. Post-combustion capture. https://www.sciencedirect.com/topics/engineering/post-combustion-capture. Reading date: 16.02.21.

[11] W. Tielin. Degradation of aqueous 2- amino-2-methyl-1-propanol for carbon dioxide capture. *Telemark University College, Norway*, PhD Thesis, 2012. doi: https://openarchive.usn.no/usn-xmlui/bitstream/handle/11250/2437799/PhD_Thesis.pdf?sequence=1&isAllowed=y.

[12] Yusoff R. Islam, M. S. and Ali B. S. Degradation studies of amines and alkanolamines during co2 absorption and stripping system. *Engineering e-Transaction*, 5:97–109, 2010.

[13] E.S. Rao and E.S. Rubin. A technical, economic, and environmental assessment of amine-based co2 capture technology for power plant greenhouse gas control. *Industrial Engineering Chemistry Research*, 36:4467–4475, 2002. doi: https://doi.org/10.1021/es0158861.

[14] J. Davis and G. T. Rochelle. Thermal degradation of monoethanolamine at stripper conditions. *Energy Procedia*, 1(1):327–333, 2009. doi: https://doi.org/10.1016/j.egypro.2009.01.045.

[15] G. T. Rochelle. Thermal degradation of amines for co2 capture. *Current Opinion in Chemical Engineering*, 1(2):183–190, 2012. doi: https://doi.org/10.1016/j.coche.2012.02.004.

[16] B.A. Oyenekan and Rochelle G.T. Alternative stripper configurations for co2 capture by aqueous amines. *AIChE J*, 53(12):3144–3154, 2007.

[17] Rochelle G.T. Oyenekan, B.A. Alternative stripper configurations for co2 capture by aqueous amines. *Ind. Eng. Chem. Res.*, 45(8):2457–2464, 2006.

[18] Lawal A. Stephenson P. Sidders M.Wang, M. and C. J., Ramshaw. Post-combustion co2 capture with chemical absorption: A state-of-the-art review. *Chemical Engineering Research and Design*, 89(9):1609–1624, 2011. doi: https://doi.org/10.1016/j.cherd.2010.11.005.

[19] Gomez M. D. Giraldo N. Huertas, J. I. and J. Garzón. Co2 absorbing capacity of

mea. *Journal of Chemistry*, Article ID 965015, 2015. doi: https://doi.org/10.1155/2015/965015.

[20]

[21] I. Eide-Haugmo. Environmental impacts and aspects of absorbents used for co2 capture. *Norwegian University of Science and Technology, Department of Chemical Engineering*, Philosophiae Doctor, 2011.

[22] Sapsford D. J. Zoannou, K. and A. J. Griffiths. Thermal degradation of monoethanolamine and its effect on co2capture capacity. *International Journal of Greenhouse Gas Control*, 17:423–430, 2013. doi: https://doi.org/10.1016/j.ijggc.2013.05.026.

[23] Grimstvedt A. Knuutila H. Fytianos, G. and H. F. Svendsen. Effect of mea's degradation products on corrosion at co2 capture plants. *Energy Procedia*, 63:1869–1875, 2014. doi: 10.1016/j.egypro.2014.11.195.

[24] Zhu R. Brunelli N. A. Sholl D. S. Didas, S. A. and C. W. Jones. Thermal, oxidative and co2 induced degradation of primary amines used for co2 capture: Effect of alkyl linker on stability. *Physical Chemistry*, 23(118):12302–12311, 2014. doi: https://doi.org/10.1021/jp5025137.

[25] T. Chai and Draxler R. R. Root mean square error (rmse) or mean absolute error (mae)? – arguments against avoiding rmse in the literature. *Geoscientific Model Development*, 7:1247–1250, 2014.

[26] Vevelstad S. J. Fytianos, G. and H. Knuutila. Corrosion and degradation in mea based post-combustion co2 capture. *International Journal of Greenhouse Gas Control*, 50:240–247, 2016. doi: 10.1016/j.ijggc.2016.05.003.

[27] P. Tontiwachwuthikul and R. Idem. Recent progress and new developments in post-combustion carbon-capture technology with reactive solvents. *Future Science*, 2013. doi: https://doi.org/10.2217/ebo.13.388.

[28] Fernandez-Luna J. M. Cleger-Tamayo, S. and Huete J. On the use of weighted mean absolute error in recommender systems. In *RUE@RecSys*, 2012.

[29] Jin J.-Eimer D. A. Han, J. and M. C. Melaaen. Density of water (1) + monoethanolamine (2) + co2 (3) from (298.15 to 413.15) k and surface tension of water (1) + monoethanolamine (2) from (303.15 to 333.15) k. *JOURNAL OF CHEMICAL ENGINEERING DATA*, 57(4):1095–1103, 2012. doi: 10.1021/je2010038.

[30] Corless G. H. Gonnet D. E. G. Hare D. J. Jeffrey Robert, M. and D. E. Knuth. On the lambert w function. *Advances in Computational Mathematics*, 5:329–359, 1996. doi: 10.1007/BF02124750.

Appendices

Appendix A

Calculating the initial MEA concentration

All calculations are performed for inital MEA solutions of 30wt% MEA. The calculations below is an example calculation performed for 0.4 mol CO_2 per mol MEA, but same procedure is used for all loadings.

$$\frac{300 \text{ g MEA/kg unloaded sol}}{61 \text{ g/mol}} = 4.9 \frac{\text{mol MEA}}{\text{kg unloaded sol}}$$

$$0.4 \frac{\text{mol } CO_2}{\text{mol MEA}} \cdot 4.9 \frac{\text{mol MEA}}{\text{kg unloaded sol}} = 1.96 \frac{\text{mol } CO_2}{\text{kg unloaded sol}}$$

$$300 \text{ g MEA} + 700 \text{ g } H_2O + 1.96 \frac{\text{mol } CO_2}{\text{kg unloaded sol}} \cdot 44 \frac{\text{g } CO_2}{\text{mol}} = 1086 \text{ g loaded solution}$$

$$4.9 \frac{\text{mol MEA}}{\text{kg unloaded sol}} \cdot \frac{1 \text{ kg unloaded sol}}{1.086 \text{ kg loaded sol}} = 4.52 \frac{\text{mol MEA}}{\text{kg loaded sol}}$$

$$4.52 \frac{\text{mol MEA}}{\text{kg loaded sol}} \cdot 1089,5 \frac{\text{kg loaded sol}}{\text{L loaded sol}} = 4,93 \frac{\text{mol MEA}}{\text{L loaded sol}}$$

Where 1089,5 is the solution density for loading 0.4.

Appendix B

Unit Conversion Calculations

Mol/100g to molarity

The data by Leonard was given in mol/100g. The data was converted into molarity by equation B.

$$\frac{mol}{100g} \cdot \frac{1000g}{kg} \cdot \rho\left(\frac{kg}{L}\right) = \frac{mol}{l}$$

Where ρ (kg/L) represents the densities at the different CO_2 loadings, given in literature [29]. The solutions are cooled down before analysis, so all densities were found at room temperature.

Mg/L to mol/L

The data from one of the experiments by Fytianos was given in mg/L, and is converted to molarity by Equation B.

$$\frac{mg}{L} \cdot \frac{1}{Mm}\left(\frac{mol}{1000mg}\right) = \frac{mol}{l}$$

Where Mm is the molar mass of the different compounds, given in g/mol.

% from Nitrogen balance to mol/L

Zoannaou performed a nitrogen balance, so the amounts of MEA and the degradation products are given as a percentage of the inital Nitrogen concentration. As MEA holds one Nitrogen atom, the initial concentration of MEA reflects the initial nitrogen concentration. From there, the percentage given for each component, combined stochiometry of nitrogen atoms, are used to calculate the associated concentrations. This is given by Equation B.0.1.

$$\frac{1}{\nu} \cdot C_{MEA,0} \left(\frac{mol}{l} \right) \cdot \frac{\%}{100\%} = \frac{mol}{l} \tag{B.0.1}$$

Where ν is the number of Nitrogen atoms in the current component.

Molality to molarity

The data given in molality is converted as described here.

$$m \frac{\text{mol MEA}}{\text{kg loaded sol}} \cdot \rho \frac{\text{kg loaded sol}}{\text{L loaded sol}} = \frac{\text{mol MEA}}{\text{L loaded sol}}$$

Appendix C

The Complete Set of Plots

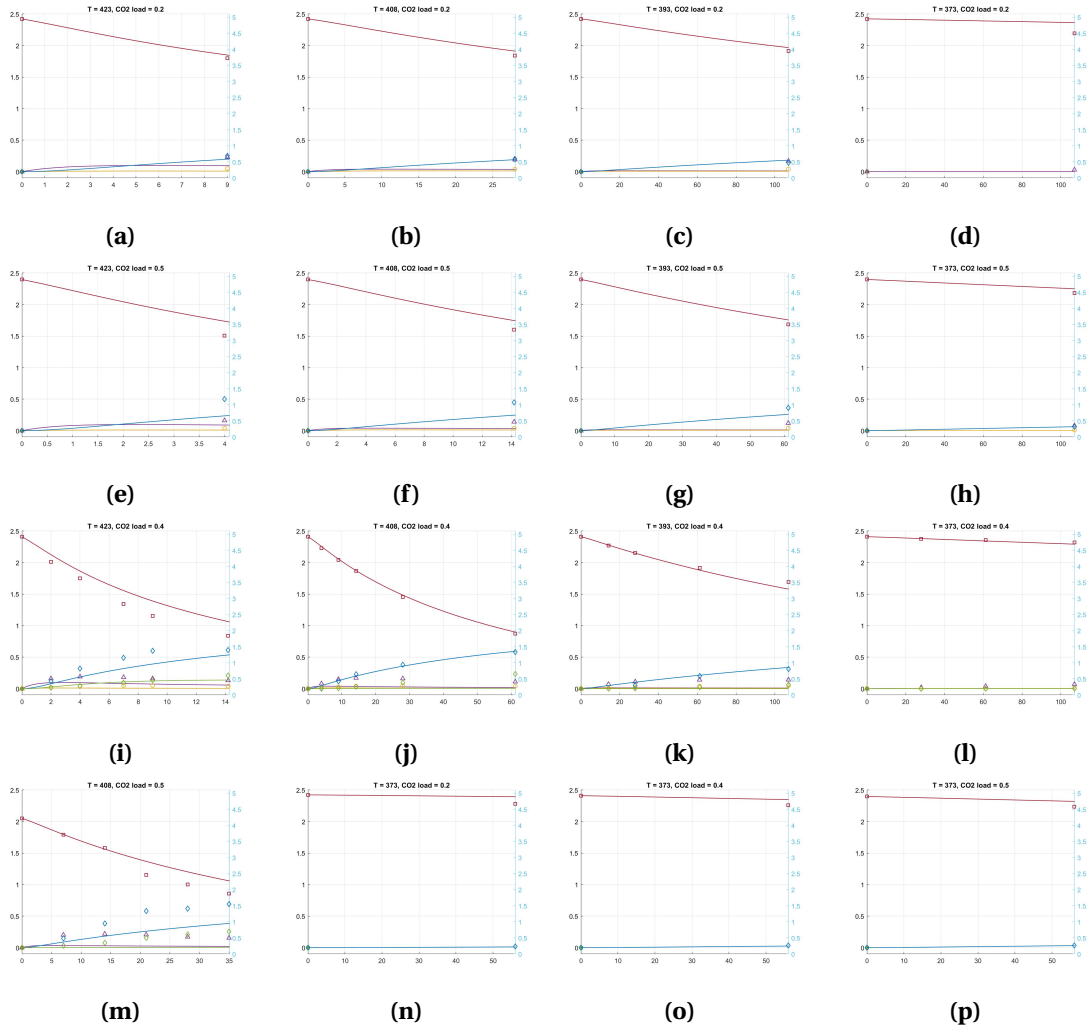

Figure C.0.1

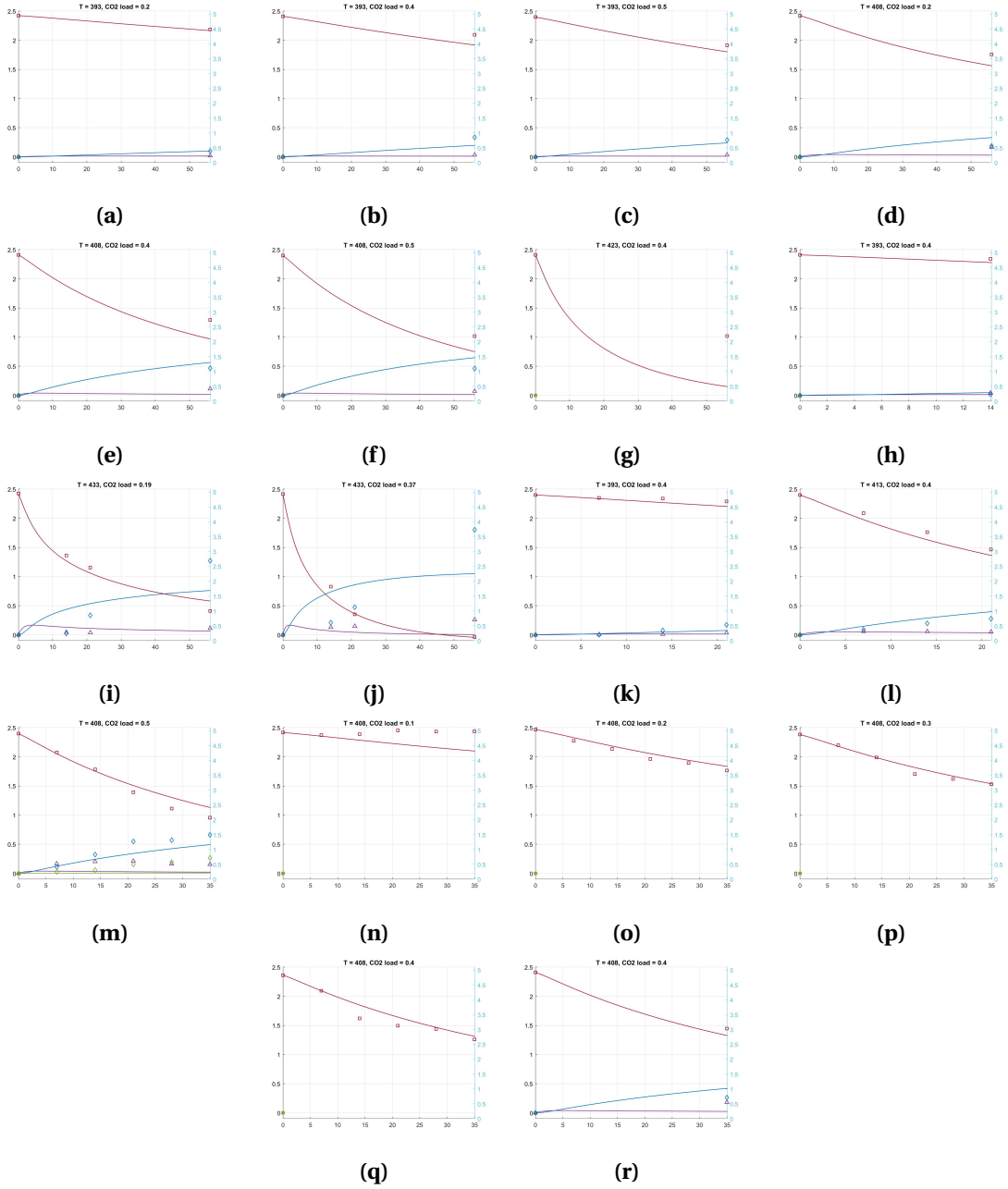

(a) **(b)** **(c)** **(d)**

(e) **(f)** **(g)** **(h)**

(i) **(j)** **(k)** **(l)**

(m) **(n)** **(o)** **(p)**

(q) **(r)**

Figure C.0.2

Appendix D

Values for TriHEIA

Table D.0.1: Experimental TriHEIA values used in the recreation of Davis' Model.

Temp	Loading	Time	Exp
100	0.4	28	0.00081
100	0.4	61.2	0.00049
100	0.4	107	0.00132
120	0.4	14.2	0.002
120	0.4	28	0.004
120	0.4	61.2	0.024
120	0.4	107	0.067
135	0.4	4	0.005
135	0.4	9	0.008
135	0.4	14.2	0.03
135	0.4	28	0.097
135	0.4	61.2	0.234
150	0.4	2	0.014
150	0.4	4	0.041
150	0.4	7	0.095
150	0.4	9	0.132
150	0.4	14.2	0.209

Appendix E

ODE Solvers

The syntax of the ODE solvers is given as follows.

[t,C] = ode23s(odefun,tspan,C0)

The first input argument, *odefun*, is the ODE function(s) to be solved, which in this case are the differential equations in the kinetic model. The second input argument, *tspan*, is the time span from t_0 to t_{final}, referring to the duration of the experiments. The initial conditions, *y0*, was defined as a vector of the initial concentrations of MEA and the degradation products. The ODE solver integrates the system of differential equations from t_0 to t_{final}. The output is a solution array, [t,C], corresponding to the concentration profiles given by the recreated model.

The built-in Matlab solver, *ode23s*, solve stiff differential equations. Differential equation problems are called stiff if the solution varies slowly, but there are nearby solutions that vary rapidly, necessitating small steps to find satisfactory results. Essentially, stiffness is only an efficiency issue. Non-stiff solvers also find the solution but are more time-consuming if the problem is stiff [30]. The non-stiff solver, *ode45*, which was used when recreating the model by Davis, was also tested in the code development, but *ode23s* was proved to be more efficient for this case. Thus, *ode23s* is preferred in the final model due to efficiency.

Appendix F

Table of average relative and absolute errors

The average absolute and relative errors were calculated by Equation 4.3.1 for each component in the models. The results are used spot trends of model over- or underestimation. The results are tabulated in Table F.0.1.

Table F.0.1: Average of the absolute deviation for all the experimental points used in each model.

		MEA	HEEDA	Trimer	HEIA	TriHEIA
Data and constants by Davis	**Abs Err**	0.0624	-0.0016	-0.0016	-0.0165	-0.0054
	Rel Err	0.0185	0.0010	-0.1109	-0.1227	-0.1285
All data with Davis const	**Abs Err**	-0.0419	0.0072	-0.0016	-0.0308	-0.0054
	Rel Err	-0.0397	0.6580	-0.1109	0.2660	-0.1285
All data with opt const	**Abs Err**	0.0011	-0.0510	-0.0151	-0.0120	-0.0230
	Rel Err	0.0033	-0.5770	-0.6731	0.3840	-0.5796

Appendix G

Matlab Code

G.1 Main

```
%MAIN
clear,clc;

%set initial exponents for the parameters
x = [-1.8 -1.0 -1.2 -0.7 -1.5 -0.5 -1.5 5 5 5 5 5 5 5];

%% experimental values:
exp_MEA = Cell_array_MEA();
exp_HEEDA = Cell_array_HEEDA();
exp_Trimer = Cell_array_Trimer();
exp_HEIA = Cell_array_HEIA();
exp_triHEIA = Cell_array_triHEIA();

%% tspan
tspan = linspace(0,115,1001);

%% Initial
C_init = [4.9 0 0 0 0 0 2.0];
T = 400;

%% Find optimal model parameters
x_opt = optimisation(x,exp_MEA,exp_HEEDA,exp_Trimer,exp_HEIA,exp_triHEIA);

%% Plotting
plotting(tspan,exp_MEA,exp_HEEDA,exp_HEIA,exp_Trimer,exp_triHEIA,x_opt);
```

G.2 Optimisation

```
%OPTIMISATION
function xopt = optimisation(x,exp_MEA,exp_HEEDA,exp_Trimer,exp_HEIA, exp_triHEIA
    )
    options=optimset('Display','iter','MaxFunEvals',1);

    p = 14;
    opts = optimoptions('particleswarm');
    opts.Display = 'iter';
    opts.UseParallel = true;
    opts.FunctionTolerance = 1e-4;
    opts.SwarmSize = 10*p;
    opts.MaxStallIterations = 10;

    %%%% k1     k2     k3     k4     k_4    k5    k_5       Ea1  Ea2  Ea3
    lb = [-3.2  -1.8   -2.5      -1.5   -5.6   -2.9   -2.0          4.5  3.8
        3.9  4.1 3.0      4.5  3.8];
    ub = [-1.6  -0.01  -0.01  -0.01      -1.3   -0.01  -0.3          5.3  5.2
        5.2  5.2 5.3      5.8  5.3];
```

```
16
17      xopt = particleswarm(@(x) object_function(x,exp_MEA,exp_HEEDA,exp_Trimer,
            exp_HEIA, exp_triHEIA),p,lb,ub,opts);
18  end
```

G.3 Objective Function

```
1   %OBJECT FUNCTION
2   function RMSE = object_function(x,exp_MEA,exp_HEEDA,exp_Trimer,exp_HEIA,
        exp_triHEIA)
3
4   m = 0;
5   RMSE_num = 0;
6
7   %% Go through all experiments to add each Prediction error to total RMSE
8   for i = 1:size(exp_MEA,1)
9       T = exp_MEA{i,3};
10      C_init_MEA = exp_MEA{i,2}(1);
11      CO2_load=exp_MEA{i,4};
12      CO2_H2O = CO2_load*C_init_MEA;
13      t_exp_MEA = exp_MEA{i,1};
14
15      %Initial conditions for ODE solver
16      C_init = [C_init_MEA 0 0 0 0 0 CO2_H2O];
17
18      %Set manual high value for RMSE when rate constants are too high for
19      %the ODE to solve the system of equations
20      warning("");
21      C_mod_mat = odefun(t_exp_MEA,C_init,x,T);
22
23      if lastwarn ~= ""
24          RMSE = 100;
25          return
26      end
27
28      if length(t_exp_MEA) <= 2
29          C_mod_mat = [C_mod_mat(1,:); C_mod_mat(end,:)];
30      end
31
32      %MEA
33      C_exp_MEA = exp_MEA{i,2};
34      C_mod_MEA = C_mod_mat(:,1);
35
36      if all(C_mod_MEA == C_mod_MEA(1))  %(~= did not work)
37      else
38          m = m + length(t_exp_MEA);
39          RMSE_num = RMSE_num + sum((C_mod_MEA'-C_exp_MEA).^2);
40      end
```

```
41
42      %HEEDA
43      C_exp_HEEDA = exp_HEEDA{i,2};
44      C_mod_HEEDA = C_mod_mat(:,2);
45
46      if all(C_mod_HEEDA == C_mod_HEEDA(1))
47      else
48          m = m + length(t_exp_MEA);
49          RMSE_num = RMSE_num + sum((C_mod_HEEDA'-C_exp_HEEDA).^2);
50      end
51
52      %Trimer
53      C_exp_Trimer = exp_Trimer{i,2};
54      C_mod_Trimer = C_mod_mat(:,3);
55
56      if all(C_mod_Trimer == C_mod_Trimer(1))
57      else
58          m = m + length(t_exp_MEA);
59          RMSE_num = RMSE_num + sum((C_mod_Trimer'-C_exp_Trimer).^2);
60      end
61
62      %HEIA
63      C_exp_HEIA = exp_HEIA{i,2};
64      C_mod_HEIA = C_mod_mat(:,5);
65
66      if all(C_mod_HEIA == C_mod_HEIA(1))
67      else
68          m = m + length(t_exp_MEA);
69          RMSE_num = RMSE_num + sum((C_mod_HEIA'-C_exp_HEIA).^2);
70      end
71
72      %TriHEIA
73      C_exp_triHEIA = exp_triHEIA{i,2};
74      C_mod_triHEIA = C_mod_mat(:,6);
75
76      if all(C_mod_triHEIA == C_mod_triHEIA(1))
77      else
78          m = m + length(t_exp_MEA);
79          RMSE_num = RMSE_num + sum((C_mod_triHEIA'-C_exp_triHEIA).^2);
80      end
81
82  end
83
84    %Total Error
85      p=14;
86      RMSE = sqrt((RMSE_num)/(m-p));
87
88
```

```
end
```

G.4 ODE Solver

```
%ODE FUNCTION
function C = odefun(tspan,C_init,x,T)
[~,C] = ode23s(@(t,C) model(t,C,x,T), tspan, C_init);
end
```

G.5 Model

```
%MODEL FUNCTION
function dC = model(t,C,x,T)

R = 8.314;
Tref = 400;

kr1 =  10^x(1);
kr2 =  10^x(2);
kr3 =  10^x(3);
kr4 =  10^x(4);
kr_4 = 10^x(5);
kr5 =  10^x(6);
kr_5 = 10^x(7);

Ea1 =  10^x(8);
Ea2 =  10^x(9);
Ea3 =  10^x(10);
Ea4 =  10^x(11);
Ea_4 = 10^x(12);
Ea5 =  10^x(13);
Ea_5 = 10^x(14);

k1  = kr1*exp(-Ea1/R * (1/T - 1/Tref));
k2  = kr2*exp(-Ea2/R * (1/T - 1/Tref));
k3  = kr3*exp(-Ea3/R * (1/T - 1/Tref));
k4  = kr4*exp(-Ea4/R * (1/T - 1/Tref));
k_4 = kr_4*exp(-Ea_4/R * (1/T - 1/Tref));
k5  = kr5*exp(-Ea5/R * (1/T - 1/Tref));
k_5 = kr_5*exp(-Ea_5/R * (1/T - 1/Tref));

%  1       2         3        4       5       6          7
%('MEA','HEEDA','TRIMEA','POLY','HEIA','TRIHEIA','CO2')

dC = zeros(7,1);
dC(1) = -2*k1*C(1)*C(7) - k2*C(2)*C(7) - k3*C(3)*C(7);
dC(2) = k1*C(1)*C(7) - k2*C(2)*C(7) - k4*C(2)*C(7) + k_4*C(5);
dC(3) = k2*C(2)*C(7) - k3*C(3)*C(7) - k5*C(3)*C(7) - k_5*C(6);
```

```
dC(4) = k3*C(3)*C(7);
dC(5) = k4*C(2)*C(7) - k_4*C(5);
dC(6) = k5*C(3)*C(7) - k_5*C(6);
dC(7) = k_4*C(5) - k4*C(2)*C(7) + k_5*C(6) - k5*C(3)*C(7);

end
```

G.6 Experimental values - MEA

```
%EXPERIMENTAL

function C = Cell_array_MEA()

    %Rochelle, 0.2
    time1 = [0 9];
    data1 = [4.951 3.73];
    T1 = 423;
    load1 = 0.2;

    time2 = [0 28];
    data2 = [4.951 3.81];
    T2 = 408;
    load2 = 0.2;

    time3 = [0 107];
    data3 = [4.951 3.95];
    T3 = 393;
    load3 = 0.2;

    time4 = [0 107];
    data4 = [4.951 4.5];
    T4 = 373;
    load4 = 0.2;


    %0.5
    time5 = [0 4];
    data5 = [4.899 3.15];
    T5 = 423;
    load5 = 0.5;

    time6 = [0 14.2];
    data6 = [4.899 3.34];
    T6 = 408;
    load6 = 0.5;

    time7 = [0 61.2];
    data7 = [4.899 3.5];
```

```
T7 = 393;
load7 = 0.5;

time8 = [0 107];
data8 = [4.899 4.48];
T8 = 373;
load8 = 0.5;


%0.4
time9 = [0 2 4 7 9 14.2];
data9 = [4.925 4.14 3.63 2.83 2.46 1.84];
T9 = 423;
load9 = 0.4;

time10 = [0 4 9 14.2 28 61.2];
data10 = [4.925 4.57 4.2 3.86 3.05 1.91];
T10 = 408;
load10 = 0.4;

time11 = [0 14.2 28 61.2 107];
data11 = [4.925 4.65 4.42 3.96 3.52];
T11 = 393;
load11 = 0.4;

time12 = [0 28 61.2 107];
data12 = [4.925 4.86 4.82 4.75];
T12 = 373;
load12 = 0.4;


%EIDE-HAUGMO

time13 = [0 7 14 21 28 35];
data13 = [4.22 3.71 3.3 2.46 2.16 1.88];
T13 = 408;
load13 = 0.5;


%DAVIS&ROCHELLE
%100deg
time14 = [0 56];
data14 = [4.951 4.670];
T14 = 373;
load14 = 0.2;

time15 = [0 56];
data15 = [4.925 4.624];
```

```
T15 = 373;
load15 = 0.4;

time16 = [0 56];
data16 = [4.899 4.583];
T16 = 373;
load16 = 0.5;

%120deg
time17 = [0 56];
data17 = [4.951 4.487];
T17 = 393;
load17 = 0.2;

time18 = [0 56];
data18 = [4.925 4.306];
T18 = 393;
load18 = 0.4;

time19 = [0 56];
data19 = [4.899 3.951];
T19 = 393;
load19 = 0.5;

%135deg
time20 = [0 56];
data20 = [4.951 3.647];
T20 = 408;
load20 = 0.2;

time21 = [0 56];
data21 = [4.925 2.735];
T21 = 408;
load21 = 0.4;

time22 = [0 56];
data22 = [4.899 2.192];
T22 = 408;
load22 = 0.5;

%150deg
time23 = [0 56];
data23 = [4.925 2.192];
T23 = 423;
load23 = 0.4;


%FYTIANOS 2
```

```
time25 = [0 14];
data25 = [4.925 4.791];
T25 = 393;
load25 = 0.4;



%Zoannou
time26 = [0 14 21 56];
data26 = [4.952      2.87150 2.45783 0.99992];
T26 = 433;
load26 = 0.19;

time27 = [0 14 21 56];
data27 = [4.931      1.81677 0.88984 0.12359];
T27 = 433;
load27 = 0.37;



%LEONARD
%120
time28 = [0 7 14 21];
data28 = [4.90275 4.804695 4.782905 4.68485];
T28 = 393;
load28 = 0.4;

%140
time29 = [0 7 14 21];
data29 = [4.903      4.293    3.650    3.072];
T29 = 413;
load29 = 0.4;


%Lepaumier
time30 = [0 7 14 21 28 35];
data30 = [4.8993'    4.2683' 3.6965' 2.9321' 2.3752' 2.0711'];
T30 = 408;
load30 = 0.5;

%Eide-Haugmo
time31 = [0 7 14 21 28 35];
data31 = [4.94 4.85 4.88 5.01 4.97 4.98];
T31 = 408;
load31 = 0.1;

time32 = [0 7 14 21 28 35];
data32 = [5.04 4.66 4.39 4.05 3.91 3.66];
```

```
T32 = 408;
load32 = 0.2;

time33 = [0 7 14 21 28 35];
data33 = [4.87 4.51 4.10 3.54 3.38 3.20];
T33 = 408;
load33 = 0.3;

time34 = [0 7 14 21 28 35];
data34 = [4.83 4.31 3.38 3.13 3.02 2.67];
T34 = 408;
load34 = 0.4;


%FYTIANOS
time35 = [0 35];
data35 = [4.925 3.0361];
T35 = 408;
load35 = 0.4;


C = {time1,data1,T1,load1;
     time2,data2,T2,load2;
     time3,data3,T3,load3;
     time4,data4,T4,load4;
     time5,data5,T5,load5;
     time6,data6,T6,load6;
     time7,data7,T7,load7;
     time8,data8,T8,load8;
     time9,data9,T9,load9;
     time10,data10,T10,load10;
     time11,data11,T11,load11;
     time12,data12,T12,load12;
     time13,data13,T13,load13;
     time14,data14,T14,load14;
     time15,data15,T15,load15;
     time16,data16,T16,load16;
     time17,data17,T17,load17;
     time18,data18,T18,load18;
     time19,data19,T19,load19;
     time20,data20,T20,load20;
     time21,data21,T21,load21;
     time22,data22,T22,load22;
     time23,data23,T23,load23;
     time25,data25,T25,load25;
     time26,data26,T26,load26;
     time27,data27,T27,load27;
     time28,data28,T28,load28;
```

```
            time29,data29,T29,load29;
            time30,data30,T30,load30;
            time31,data31,T31,load31;
            time32,data32,T32,load32;
            time33,data33,T33,load33;
            time34,data34,T34,load34;
            time35,data35,T35,load35;
        };


end
```

G.7 Experimental values - HEEDA

```
%EXPERIMENTAL HEEDA

function C = Cell_array_HEEDA()

    %ROCHELLE (TEXAS).

    %Rochelle, 0.2
    time1 = [0 9];
    data1 = [0 0.23];
    T1 = 423;
    load1 = 0.2;

    time2 = [0 28];
    data2 = [0 0.19];
    T2 = 408;
    load2 = 0.2;

    time3 = [0 107];
    data3 = [0 0.17];
    T3 = 393;
    load3 = 0.2;

    time4 = [0 107];
    data4 = [0 0.03];
    T4 = 373;
    load4 = 0.2;


    %0.5
    time5 = [0 14];
    data5 = [0 0.16];
    T5 = 423;
    load5 = 0.5;

```

```
time6 = [0 14.2];
data6 = [0 0.14];
T6 = 408;
load6 = 0.5;

time7 = [0 61.2];
data7 = [0 0.12];
T7 = 393;
load7 = 0.5;

time8 = [0 107];
data8 = [0 0.08];
T8 = 373;
load8 = 0.5;


%0.4
time9 = [0 2 4 7 9 14.2];
data9 = [0 0.16 0.19 0.18 0.16 0.13];
T9 = 423;
load9 = 0.4;

time10 = [0 4 9 14.2 28 61.2];
data10 = [0 0.08 0.15 0.17 0.16 0.11];
T10 = 408;
load10 = 0.4;

time11 = [0 14.2 28 61.2 107];
data11 = [0 0.07 0.11 0.14 0.14];
T11 = 393;
load11 = 0.4;

time12 = [0 28 61.2 107];
data12 = [0 0.02 0.04 0.07];
T12 = 473;
load12 = 0.4;



%EIDE-HAUGMO
time13 = [0 7 14 21 28 35];
data13 = [0 0.2025 0.2171 0.2064 0.1719 0.1548];
T13 = 408;
load13 = 0.5;



%TEXAS DAVIS
```

```
%100deg
time14 = [0 56];
data14 = [0 0];
T14 = 373;
load14 = 0.2;

time15 = [0 56];
data15 = [0 0];
T15 = 373;
load15 = 0.4;

time16 = [0 56];
data16 = [0 0];
T16 = 373;
load16 = 0.5;

%120deg
time17 = [0 56];
data17 = [0 0.020];
T17 = 393;
load17 = 0.2;

time18 = [0 56];
data18 = [0 0.033];
T18 = 393;
load18 = 0.4;

time19 = [0 56];
data19 = [0 0.033];
T19 = 393;
load19 = 0.5;

%135deg
time20 = [0 56];
data20 = [0 0.165];
T20 = 408;
load20 = 0.2;

time21 = [0 56];
data21 = [0 0.113];
T21 = 408;
load21 = 0.4;

time22 = [0 56];
data22 = [0 0.073];
T22 = 408;
load22 = 0.5;

```

```
%150deg
time23 = [0 56];
data23 = [0 0];
T23 = 423;
load23 = 0.4;

%FYTIANOS 2
time25 = [0 14];
data25 = [0 0.044167];
T25 = 393;
load25 = 0.4;

%Zoannou
time26 = [0 14 21 56];
data26 = [0 0.04492 0.03932 0.11358];
T26 = 433;
load26 = 0.19;

time27 = [0 14 21 56];
data27 = [0 0.12977 0.14831 0.25953];
T27 = 433;
load27 = 0.37;



%LEONARD
%120
time28 = [0 7 14 21];
data28 = [0 0.0075 0.0118 0.0342];
T28 = 393;
load28 = 0.4;

%140
time29 = [0 7 14 21];
data29 = [0 0.060 0.059 0.051];
T29 = 413;
load29 = 0.4;


%Lepaumier
time30 = [0 7 14 21 28 35];
data30 = [0 0.1670 0.2041 0.2116 0.1633 0.1559];
T30 = 408;
load30 = 0.5;

%Eide-Haugmo
time31 = [0 7 14 21 28 35];
data31 = [0 0 0 0 0 0];
```

```
T31 = 408;
load31 = 0.1;

time32 = [0 7 14 21 28 35];
data32 = [0 0 0 0 0 0];
T32 = 408;
load32 = 0.2;

time33 = [0 7 14 21 28 35];
data33 = [0 0 0 0 0 0];
T33 = 408;
load33 = 0.3;

time34 = [0 7 14 21 28 35];
data34 = [0 0 0 0 0 0];
T34 = 408;
load34 = 0.4;

%FYTIANOS
time35 = [0 35];
data35 = [0 0.1813];
T35 = 408;
load35 = 0.4;


C = {time1,data1,T1,load1;
     time2,data2,T2,load2;
     time3,data3,T3,load3;
     time4,data4,T4,load4;
     time5,data5,T5,load5;
     time6,data6,T6,load6;
     time7,data7,T7,load7;
     time8,data8,T8,load8;
     time9,data9,T9,load9;
     time10,data10,T10,load10;
     time11,data11,T11,load11;
     time12,data12,T12,load12;
     time13,data13,T13,load13;
     time14,data14,T14,load14;
     time15,data15,T15,load15;
     time16,data16,T16,load16;
     time17,data17,T17,load17;
     time18,data18,T18,load18;
     time19,data19,T19,load19;
     time20,data20,T20,load20;
     time21,data21,T21,load21;
     time22,data22,T22,load22;
     time23,data23,T23,load23;
```

```
            time25,data25,T25,load25;
            time26,data26,T26,load26;
            time27,data27,T27,load27;
            time28,data28,T28,load28;
            time29,data29,T29,load29;
            time30,data30,T30,load30;
            time31,data31,T31,load31;
            time32,data32,T32,load32;
            time33,data33,T33,load33;
            time34,data34,T34,load34;
            time35,data35,T35,load35;
        };



end
```

G.8 Experimental values - Trimer

```
%EXPERIMENTAL Trimer

function C = Cell_array_Trimer()

    %ROCHELLE (TEXAS).

    %0.2
    time1 = [0 9];
    data1 = [0 0.05];
    T1 = 423;
    load1 = 0.2;

    time2 = [0 28];
    data2 = [0 0.04];
    T2 = 408;
    load2 = 0.2;

    time3 = [0 107];
    data3 = [0 0.04];
    T3 = 393;
    load3 = 0.2;

    time4 = [0 107];
    data4 = [0 0];
    T4 = 373;
    load4 = 0.2;


    %0.5
```

```
30      time5 = [0 4];
31      data5 = [0 0.04];
32      T5 = 423;
33      load5 = 0.5;
34
35      time6 = [0 14.2];
36      data6 = [0 0.04];
37      T6 = 408;
38      load6 = 0.5;
39
40      time7 = [0 61.2];
41      data7 = [0 0.04];
42      T7 = 393;
43      load7 = 0.5;
44
45      time8 = [0 107];
46      data8 = [0 0.01];
47      T8 = 373;
48      load8 = 0.5;
49
50
51      %0.4
52      time9 = [0 2 4 7 9 14.2];
53      data9 = [0 0.02 0.04 0.05 0.05 0.04];
54      T9 = 423;
55      load9 = 0.4;
56
57      time10 = [0 4 9 14.2 28 61.2];
58      data10 = [0 0.01 0.03 0.04 0.05 0.04];
59      T10 = 408;
60      load10 = 0.4;
61
62      time11 = [0 14.2 28 61.2 107];
63      data11 = [0 0.01 0.02 0.04 0.05];
64      T11 = 393;
65      load11 = 0.4;
66
67      time12 = [0 28 61.2 107];
68      data12 = [0 0 0 0.01];
69      T12 = 473;
70      load12 = 0.4;
71
72    %EIDE-HAUGMO
73      time13 = [0 7 14 21 28 35];
74      data13 = [0 0 0 0 0 0];
75      T13 = 408;
76      load13 = 0.5;
77
```

```
%TEXAS  DAVIS
%100deg
time14 = [0  56];
data14 = [0  0];
T14 = 373;
load14 = 0.2;

time15 = [0  56];
data15 = [0  0];
T15 = 373;
load15 = 0.4;

time16 = [0  56];
data16 = [0  0];
T16 = 373;
load16 = 0.5;

%120deg
time17 = [0  56];
data17 = [0  0];
T17 = 393;
load17 = 0.2;

time18 = [0  56];
data18 = [0  0];
T18 = 393;
load18 = 0.4;

time19 = [0  56];
data19 = [0  0];
T19 = 393;
load19 = 0.5;

%135deg
time20 = [0  56];
data20 = [0  0];
T20 = 408;
load20 = 0.2;

time21 = [0  56];
data21 = [0  0];
T21 = 408;
load21 = 0.4;

time22 = [0  56];
data22 = [0  0];
T22 = 408;
load22 = 0.5;
```

```
126
127     %150deg
128     time23 = [0  56];
129     data23 = [0  0];
130     T23 = 423;
131     load23 = 0.4;
132
133     %FYTIANOS 2
134     time25 = [0  14];
135     data25 = [0  0];
136     T25 = 393;
137     load25 = 0.4;
138
139      %Zoannou
140     time26 = [0  14  21  56];
141     data26 = [0  0  0  0];
142     T26 = 433;
143     load26 = 0.19;
144
145     time27 = [0  14  21  56];
146     data27 = [0  0  0  0];
147     T27 = 433;
148     load27 = 0.37;
149
150
151     %LEONARD
152     %120
153     time28 = [0  7  14  21];
154     data28 = [0  0  0  0];
155     T28 = 393;
156     load28 = 0.4;
157
158     %140
159     time29 = [0  7  14  21];
160     data29 = [0  0  0  0];
161     T29 = 413;
162     load29 = 0.4;
163
164     %Lepaumier
165     time30 = [0  7  14  21  28  35];
166     data30 = [0  0  0  0  0  0];
167     T30 = 408;
168     load30 = 0.5;
169
170     %Eide-Haugmo
171     time31 = [0  7  14  21  28  35];
172     data31 = [0  0  0  0  0  0];
173     T31 = 408;
```

```
load31 = 0.1;

time32 = [0 7 14 21 28 35];
data32 = [0 0 0 0 0 0];
T32 = 408;
load32 = 0.2;

time33 = [0 7 14 21 28 35];
data33 = [0 0 0 0 0 0];
T33 = 408;
load33 = 0.3;

time34 = [0 7 14 21 28 35];
data34 = [0 0 0 0 0 0];
T34 = 408;
load34 = 0.4;

%FYTIANOS
time35 = [0 35];
data35 = [0 0];
T35 = 408;
load35 = 0.4;


C = {time1,data1,T1,load1;
     time2,data2,T2,load2;
     time3,data3,T3,load3;
     time4,data4,T4,load4;
     time5,data5,T5,load5;
     time6,data6,T6,load6;
     time7,data7,T7,load7;
     time8,data8,T8,load8;
     time9,data9,T9,load9;
     time10,data10,T10,load10;
     time11,data11,T11,load11;
     time12,data12,T12,load12;
     time13,data13,T13,load13;
     time14,data14,T14,load14;
     time15,data15,T15,load15;
     time16,data16,T16,load16;
     time17,data17,T17,load17;
     time18,data18,T18,load18;
     time19,data19,T19,load19;
     time20,data20,T20,load20;
     time21,data21,T21,load21;
     time22,data22,T22,load22;
     time23,data23,T23,load23;
     time25,data25,T25,load25;
```

```
            time26,data26,T26,load26;
            time27,data27,T27,load27;
            time28,data28,T28,load28;
            time29,data29,T29,load29;
            time30,data30,T30,load30;
            time31,data31,T31,load31;
            time32,data32,T32,load32;
            time33,data33,T33,load33;
            time34,data34,T34,load34;
            time35,data35,T35,load35;
        };


end
```

G.9 Experimental values - HEIA

```
%EXPERIMENTAL HEIA

function C = Cell_array_HEIA()

    %ROCHELLE (TEXAS).

    % 0.2
    time1 = [0 9];
    data1 = [0 0.25];
    T1 = 423;
    load1 = 0.2;

    time2 = [0 28];
    data2 = [0 0.2];
    T2 = 408;
    load2 = 0.2;

    time3 = [0 107];
    data3 = [0 0.14];
    T3 = 393;
    load3 = 0.2;

    time4 = [0 107];
    data4 = [0 0];
    T4 = 373;
    load4 = 0.2;


    %0.5
    time5 = [0 4];
```

```
data5 = [0 0.5];
T5 = 423;
load5 = 0.5;

time6 = [0 14.2];
data6 = [0 0.45];
T6 = 408;
load6 = 0.5;

time7 = [0 61.2];
data7 = [0 0.36];
T7 = 393;
load7 = 0.5;

time8 = [0 107];
data8 = [0 0.06];
T8 = 373;
load8 = 0.5;


%0.4
time9 = [0 2 4 7 9 14.2];
data9 = [0 0.12 0.32 0.49 0.6 0.61];
T9 = 423;
load9 = 0.4;

time10 = [0 4 9 14.2 28 61.2];
data10 = [0 0 0.12 0.23 0.38 0.58];
T10 = 408;
load10 = 0.4;

time11 = [0 14.2 28 61.2 107];
data11 = [0 0 0.05 0.2 0.31];
T11 = 393;
load11 = 0.4;

time12 = [0 28 61.2 107];
data12 = [0 0 0 0];
T12 = 473;
load12 = 0.4;


%EIDE-HAUGMO

time13 = [0 7 14 21 28 35];
data13 = [0 0.1501 0.3822 0.5832 0.6209 0.6900];
T13 = 408;
load13 = 0.5;
```

```
79
80      %TEXAS DAVIS
81      %100deg
82      time14 = [0 56];
83      data14 = [0 0.020];
84      T14 = 373;
85      load14 = 0.2;
86
87      time15 = [0 56];
88      data15 = [0 0.034];
89      T15 = 373;
90      load15 = 0.4;
91
92      time16 = [0 56];
93      data16 = [0 0.034];
94      T16 = 373;
95      load16 = 0.5;
96
97      %120deg
98      time17 = [0 56];
99      data17 = [0 0.100];
100     T17 = 393;
101     load17 = 0.2;
102
103     time18 = [0 56];
104     data18 = [0 0.336];
105     T18 = 393;
106     load18 = 0.4;
107
108     time19 = [0 56];
109     data19 = [0 0.288];
110     T19 = 393;
111     load19 = 0.5;
112
113     %135deg
114     time20 = [0 56];
115     data20 = [0 0.186];
116     T20 = 408;
117     load20 = 0.2;
118
119     time21 = [0 56];
120     data21 = [0 0.467];
121     T21 = 408;
122     load21 = 0.4;
123
124     time22 = [0 56];
125     data22 = [0 0.465];
126     T22 = 408;
```

```
load22 = 0.5;

%150deg
time23 = [0 56];
data23 = [0 0];
T23 = 423;
load23 = 0.4;


%FYTIANOS 2
time25 = [0 14];
data25 = [0 0.016703];
T25 = 393;
load25 = 0.4;



%Zoannou
time26 = [0 14 21 56];
data26 = [0 0.02271 0.33510 1.27212];
T26 = 433;
load26 = 0.19;

time27 = [0 14 21 56];
data27 = [0 0.21012 0.47582 1.80442];
T27 = 433;
load27 = 0.37;


%LEONARD
%120
time28 = [0 7 14 21];
data28 = [0 0       0.0751755       0.1710515];
T28 = 393;
load28 = 0.4;

%140
time29 = [0 7 14 21];
data29 = [0 0.090   0.198   0.279];
T29 = 413;
load29 = 0.4;


%Lepaumier
time30 = [0 7 14 21 28 35];
data30 = [0 0.1113  0.3229  0.5456  0.5716  0.6607];
T30 = 408;
load30 = 0.5;
```

```
175
176     %Eide-Haugmo
177     time31 = [0 7 14 21 28 35];
178     data31 = [0 0 0 0 0 0];
179     T31 = 408;
180     load31 = 0.1;
181
182     time32 = [0 7 14 21 28 35];
183     data32 = [0 0 0 0 0 0];
184     T32 = 408;
185     load32 = 0.2;
186
187     time33 = [0 7 14 21 28 35];
188     data33 = [0 0 0 0 0 0];
189     T33 = 408;
190     load33 = 0.3;
191
192     time34 = [0 7 14 21 28 35];
193     data34 = [0 0 0 0 0 0];
194     T34 = 408;
195     load34 = 0.4;
196
197     %FYTIANOS
198     time35 = [0 35];
199     data35 = [0 0.264];
200     T35 = 408;
201     load35 = 0.4;
202
203
204     C = {time1,data1,T1,load1;
205          time2,data2,T2,load2;
206          time3,data3,T3,load3;
207          time4,data4,T4,load4;
208          time5,data5,T5,load5;
209          time6,data6,T6,load6;
210          time7,data7,T7,load7;
211          time8,data8,T8,load8;
212          time9,data9,T9,load9;
213          time10,data10,T10,load10;
214          time11,data11,T11,load11;
215          time12,data12,T12,load12;
216          time13,data13,T13,load13;
217          time14,data14,T14,load14;
218          time15,data15,T15,load15;
219          time16,data16,T16,load16;
220          time17,data17,T17,load17;
221          time18,data18,T18,load18;
222          time19,data19,T19,load19;
```

```
            time20,data20,T20,load20;
            time21,data21,T21,load21;
            time22,data22,T22,load22;
            time23,data23,T23,load23;
            time25,data25,T25,load25;
            time26,data26,T26,load26;
            time27,data27,T27,load27;
            time28,data28,T28,load28;
            time29,data29,T29,load29;
            time30,data30,T30,load30;
            time31,data31,T31,load31;
            time32,data32,T32,load32;
            time33,data33,T33,load33;
            time34,data34,T34,load34;
            time35,data35,T35,load35;
        };


end
```

G.10 Experimental values - TriHEIA

```
%EXPERIMENTAL triHEIA

function C = Cell_array_triHEIA()

    %ROCHELLE (TEXAS).

    %0.2
    time1 = [0 8];
    data1 = [0 0.0];
    T1 = 423;
    load1 = 0.2;

    time2 = [0 28];
    data2 = [0 0.0];
    T2 = 408;
    load2 = 0.2;

    time3= [0 112];
    data3 = [0 0.0];
    T3 = 393;
    load3 = 0.2;

    time4 = [0 112];
    data4 = [0 0.0];
    T4 = 373;
```

```
load4 = 0.2;


%0.5
time5 = [0 4];
data5 = [0 0.0];
T5 = 423;
load5 = 0.5;

time6 = [0 14];
data6 = [0 0.0];
T6 = 408;
load6 = 0.5;

time7 = [0 63];
data7 = [0 0.0];
T7 = 393;
load7 = 0.5;

time8 = [0 112];
data8 = [0 0.0];
T8 = 373;
load8 = 0.5;

%0.4
time9 = [0 2 4 7 9 14.2];
data9 = [0 0.014 0.041 0.095 0.132 0.209];
T9 = 423;
load9 = 0.4;

time10 = [0 4 9 14.2 28 61.2];
data10 = [0 0.005 0.008 0.03 0.097 0.234];
T10 = 408;
load10 = 0.4;

time11 = [0 14.2 28 61.2 107];
data11 = [0 0.002 0.004 0.024 0.067];
T11 = 393;
load11 = 0.4;

time12 = [0 28 61.2 107];
data12 = [0 0.00081 0.00049 0.00132];
T12 = 373;
load12 = 0.4;


%EIDE-HAUGMO
%time13 = [0 7 14 21 28 35];
```

```
74      %data13 = [0 0 0 0 0 0];
75      %T13 = 408;
76      %load13 = 0.5;
77
78      %EIDE-HAUGMO
79      time13 = [0 7 14 21 28 35];
80      data13 = [0 0.0328 0.0783 0.1578 0.2097 0.2547];
81      T13 = 408;
82      load13 = 0.5;
83
84  %TEXAS DAVIS
85      %100deg
86      time14 = [0 56];
87      data14 = [0 0];
88      T14 = 373;
89      load14 = 0.2;
90
91      time15 = [0 56];
92      data15 = [0 0];
93      T15 = 373;
94      load15 = 0.4;
95
96      time16 = [0 56];
97      data16 = [0 0];
98      T16 = 373;
99      load16 = 0.5;
100
101     %120deg
102     time17 = [0 56];
103     data17 = [0 0];
104     T17 = 393;
105     load17 = 0.2;
106
107     time18 = [0 56];
108     data18 = [0 0];
109     T18 = 393;
110     load18 = 0.4;
111
112     time19 = [0 56];
113     data19 = [0 0];
114     T19 = 393;
115     load19 = 0.5;
116
117     %135deg
118     time20 = [0 56];
119     data20 = [0 0];
120     T20 = 408;
121     load20 = 0.2;
```

```
122
123     time21 = [0 56];
124     data21 = [0 0];
125     T21 = 408;
126     load21 = 0.4;
127
128     time22 = [0 56];
129     data22 = [0 0];
130     T22 = 408;
131     load22 = 0.5;
132
133     %150deg
134     time23 = [0 56];
135     data23 = [0 0];
136     T23 = 423;
137     load23 = 0.4;
138
139     %FYTIANOS 2
140     time25 = [0 14];
141     data25 = [0 0];
142     T25 = 393;
143     load25 = 0.4;
144
145     %Zoannou
146     time26 = [0 14 21 56];
147     data26 = [0 0 0 0];
148     T26 = 433;
149     load26 = 0.19;
150
151     time27 = [0 14 21 56];
152     data27 = [0 0 0 0];
153     T27 = 433;
154     load27 = 0.37;
155
156   %LEONARD
157     %120
158     time28 = [0 7 14 21];
159     data28 = [0 0 0 0];
160     T28 = 393;
161     load28 = 0.4;
162
163     %140
164     time29 = [0 7 14 21];
165     data29 = [0 0 0 0];
166     T29 = 413;
167     load29 = 0.4;
168
169     %Lepaumier
```

```
%time30 = [0 7 14 21 28 35];
%data30 = [0 0 0 0 0 0];
%T30 = 408;
%load30 = 0.5;

%Lepaumier
time30 = [0 7 14 21 28 35];
data30 = [0 0.0272  0.0594  0.1571  0.1930  0.2672];
T30 = 408;
load30 = 0.5;

%Eide–Haugmo
time31 = [0 7 14 21 28 35];
data31 = [0 0 0 0 0 0];
T31 = 408;
load31 = 0.1;

time32 = [0 7 14 21 28 35];
data32 = [0 0 0 0 0 0];
T32 = 408;
load32 = 0.2;

time33 = [0 7 14 21 28 35];
data33 = [0 0 0 0 0 0];
T33 = 408;
load33 = 0.3;

time34 = [0 7 14 21 28 35];
data34 = [0 0 0 0 0 0];
T34 = 408;
load34 = 0.4;

%FYTIANOS
time35 = [0 35];
data35 = [0 0];
T35 = 408;
load35 = 0.4;


C = {time1,data1,T1,load1;
     time2,data2,T2,load2;
     time3,data3,T3,load3;
     time4,data4,T4,load4;
     time5,data5,T5,load5;
     time6,data6,T6,load6;
     time7,data7,T7,load7;
     time8,data8,T8,load8;
     time9,data9,T9,load9;
```

```
        time10,data10,T10,load10;
        time11,data11,T11,load11;
        time12,data12,T12,load12;
        time13,data13,T13,load13;
        time14,data14,T14,load14;
        time15,data15,T15,load15;
        time16,data16,T16,load16;
        time17,data17,T17,load17;
        time18,data18,T18,load18;
        time19,data19,T19,load19;
        time20,data20,T20,load20;
        time21,data21,T21,load21;
        time22,data22,T22,load22;
        time23,data23,T23,load23;
        time25,data25,T25,load25;
        time26,data26,T26,load26;
        time27,data27,T27,load27;
        time28,data28,T28,load28;
        time29,data29,T29,load29;
        time30,data30,T30,load30;
        time31,data31,T31,load31;
        time32,data32,T32,load32;
        time33,data33,T33,load33;
        time34,data34,T34,load34;
        time35,data35,T35,load35;
    };



end
```

G.11 Experimental values - TriHEIA

```
%EXPERIMENTAL triHEIA

function C = Cell_array_triHEIA()

    %ROCHELLE (TEXAS).

    %0.2
    time1 = [0 8];
    data1 = [0 0.0];
    T1 = 423;
    load1 = 0.2;

    time2 = [0 28];
    data2 = [0 0.0];
    T2 = 408;
```

```
16      load2 = 0.2;
17
18      time3= [0 112];
19      data3 = [0 0.0];
20      T3 = 393;
21      load3 = 0.2;
22
23      time4 = [0 112];
24      data4 = [0 0.0];
25      T4 = 373;
26      load4 = 0.2;
27
28
29      %0.5
30      time5 = [0 4];
31      data5 = [0 0.0];
32      T5 = 423;
33      load5 = 0.5;
34
35      time6 = [0 14];
36      data6 = [0 0.0];
37      T6 = 408;
38      load6 = 0.5;
39
40      time7 = [0 63];
41      data7 = [0 0.0];
42      T7 = 393;
43      load7 = 0.5;
44
45      time8 = [0 112];
46      data8 = [0 0.0];
47      T8 = 373;
48      load8 = 0.5;
49
50      %0.4
51      time9 = [0 2 4 7 9 14.2];
52      data9 = [0 0.014 0.041 0.095 0.132 0.209];
53      T9 = 423;
54      load9 = 0.4;
55
56      time10 = [0 4 9 14.2 28 61.2];
57      data10 = [0 0.005 0.008 0.03 0.097 0.234];
58      T10 = 408;
59      load10 = 0.4;
60
61      time11 = [0 14.2 28 61.2 107];
62      data11 = [0 0.002 0.004 0.024 0.067];
63      T11 = 393;
```

```
    load11 = 0.4;

    time12 = [0 28 61.2 107];
    data12 = [0 0.00081 0.00049 0.00132];
    T12 = 373;
    load12 = 0.4;


  %EIDE-HAUGMO
    %time13 = [0 7 14 21 28 35];
    %data13 = [0 0 0 0 0 0];
    %T13 = 408;
    %load13 = 0.5;

    %EIDE-HAUGMO
    time13 = [0 7 14 21 28 35];
    data13 = [0 0.0328 0.0783 0.1578 0.2097 0.2547];
    T13 = 408;
    load13 = 0.5;

%TEXAS DAVIS
    %100deg
    time14 = [0 56];
    data14 = [0 0];
    T14 = 373;
    load14 = 0.2;

    time15 = [0 56];
    data15 = [0 0];
    T15 = 373;
    load15 = 0.4;

    time16 = [0 56];
    data16 = [0 0];
    T16 = 373;
    load16 = 0.5;

    %120deg
    time17 = [0 56];
    data17 = [0 0];
    T17 = 393;
    load17 = 0.2;

    time18 = [0 56];
    data18 = [0 0];
    T18 = 393;
    load18 = 0.4;

```

```
112     time19 = [0 56];
113     data19 = [0 0];
114     T19 = 393;
115     load19 = 0.5;
116
117     %135deg
118     time20 = [0 56];
119     data20 = [0 0];
120     T20 = 408;
121     load20 = 0.2;
122
123     time21 = [0 56];
124     data21 = [0 0];
125     T21 = 408;
126     load21 = 0.4;
127
128     time22 = [0 56];
129     data22 = [0 0];
130     T22 = 408;
131     load22 = 0.5;
132
133     %150deg
134     time23 = [0 56];
135     data23 = [0 0];
136     T23 = 423;
137     load23 = 0.4;
138
139     %FYTIANOS 2
140     time25 = [0 14];
141     data25 = [0 0];
142     T25 = 393;
143     load25 = 0.4;
144
145     %Zoannou
146     time26 = [0 14 21 56];
147     data26 = [0 0 0 0];
148     T26 = 433;
149     load26 = 0.19;
150
151     time27 = [0 14 21 56];
152     data27 = [0 0 0 0];
153     T27 = 433;
154     load27 = 0.37;
155
156   %LEONARD
157     %120
158     time28 = [0 7 14 21];
159     data28 = [0 0 0 0];
```

```
T28 = 393;
load28 = 0.4;

%140
time29 = [0 7 14 21];
data29 = [0 0 0 0];
T29 = 413;
load29 = 0.4;

%Lepaumier
%time30 = [0 7 14 21 28 35];
%data30 = [0 0 0 0 0 0];
%T30 = 408;
%load30 = 0.5;

%Lepaumier
time30 = [0 7 14 21 28 35];
data30 = [0 0.0272  0.0594  0.1571  0.1930  0.2672];
T30 = 408;
load30 = 0.5;

%Eide-Haugmo
time31 = [0 7 14 21 28 35];
data31 = [0 0 0 0 0 0];
T31 = 408;
load31 = 0.1;

time32 = [0 7 14 21 28 35];
data32 = [0 0 0 0 0 0];
T32 = 408;
load32 = 0.2;

time33 = [0 7 14 21 28 35];
data33 = [0 0 0 0 0 0];
T33 = 408;
load33 = 0.3;

time34 = [0 7 14 21 28 35];
data34 = [0 0 0 0 0 0];
T34 = 408;
load34 = 0.4;

%FYTIANOS
time35 = [0 35];
data35 = [0 0];
T35 = 408;
load35 = 0.4;

```

```
208
209     C = {time1,data1,T1,load1;
210          time2,data2,T2,load2;
211          time3,data3,T3,load3;
212          time4,data4,T4,load4;
213          time5,data5,T5,load5;
214          time6,data6,T6,load6;
215          time7,data7,T7,load7;
216          time8,data8,T8,load8;
217          time9,data9,T9,load9;
218          time10,data10,T10,load10;
219          time11,data11,T11,load11;
220          time12,data12,T12,load12;
221          time13,data13,T13,load13;
222          time14,data14,T14,load14;
223          time15,data15,T15,load15;
224          time16,data16,T16,load16;
225          time17,data17,T17,load17;
226          time18,data18,T18,load18;
227          time19,data19,T19,load19;
228          time20,data20,T20,load20;
229          time21,data21,T21,load21;
230          time22,data22,T22,load22;
231          time23,data23,T23,load23;
232          time25,data25,T25,load25;
233          time26,data26,T26,load26;
234          time27,data27,T27,load27;
235          time28,data28,T28,load28;
236          time29,data29,T29,load29;
237          time30,data30,T30,load30;
238          time31,data31,T31,load31;
239          time32,data32,T32,load32;
240          time33,data33,T33,load33;
241          time34,data34,T34,load34;
242          time35,data35,T35,load35;
243        };
244
245
246
247 end
```

G.12 Plotting

```
1 function plotting(tspan,exp_MEA,exp_HEEDA,exp_HEIA,exp_Trimer,exp_triHEIA,x)
2 n = length(exp_MEA);
3
4 tot_exp_val = 0;
5
```

```
%% Count length of experimental values to decide size of vectors for plotting
for i = 1:n
    tot_exp_val = tot_exp_val + length(exp_MEA{i,2}) + length(exp_HEEDA{i,2}) +
        length(exp_Trimer{i,2}) + length(exp_HEIA{i,2}) + length(exp_triHEIA{i,2})
        ; %Total number of experimental values
end
exp_val_comp = tot_exp_val/5; %Number of experimental values for each component

%% Preallocating Space for Plotting Arrays
abs_err_mod_MEA = zeros(1,exp_val_comp);
rel_err_mod_MEA = zeros(1,exp_val_comp);
abs_err_mod_HEEDA = zeros(1,exp_val_comp);
rel_err_mod_HEEDA = zeros(1,exp_val_comp);
abs_err_mod_HEIA = zeros(1,exp_val_comp);
rel_err_mod_HEIA = zeros(1,exp_val_comp);
abs_err_mod_Trimer = zeros(1,exp_val_comp);
rel_err_mod_Trimer = zeros(1,exp_val_comp);
abs_err_mod_triHEIA = zeros(1,exp_val_comp);
rel_err_mod_triHEIA = zeros(1,exp_val_comp);

abs_err_tot = zeros(1,tot_exp_val);
rel_err_tot = zeros(1,tot_exp_val);

T_tot = zeros(1,tot_exp_val);
T_comp = zeros(1,exp_val_comp);
load_tot = zeros(1,tot_exp_val);
load_comp = zeros(1,exp_val_comp);
time_tot = zeros(1,tot_exp_val);
time_comp = zeros(1,exp_val_comp);
exp_tot = zeros(1,tot_exp_val);
exp_comp_MEA = zeros(1,exp_val_comp);
exp_comp_HEEDA = zeros(1,exp_val_comp);
exp_comp_trimer = zeros(1,exp_val_comp);
exp_comp_HEIA = zeros(1,exp_val_comp);
exp_comp_triHEIA = zeros(1,exp_val_comp);


%% Counting to add data at the right space in Plotting Arrays
count2 = 0;
count3 = 0;

%% Go through all the experiments
for i = 1:n
    t_exp_MEA = exp_MEA{i,1};
    y_exp_MEA = exp_MEA{i,2};
    y_init_MEA = y_exp_MEA(1);
    T = exp_MEA{i,3};
    CO2_load=exp_MEA{i,4};
```

```
52      CO2 = CO2_load*y_init_MEA;
53      C_init = [y_init_MEA 0 0 0 0 0 CO2];
54      y_exp_HEEDA = exp_HEEDA{i,2};
55      y_exp_HEIA = exp_HEIA{i,2};
56      y_exp_triHEIA = exp_triHEIA{i,2};
57      y_exp_Trimer = exp_Trimer{i,2};
58      y_mod = odefun(tspan,C_init,x,T);
59
60      % Plot modeled and experimental value
61      figure(i);
62      plotting_mod(tspan, y_mod, t_exp_MEA, y_exp_MEA, y_exp_HEEDA, y_exp_HEIA,
            y_exp_Trimer, y_exp_triHEIA, T, CO2_load);
63      hold on;
64
65      % Allocate space for abs and rel arrays for each point in experiment
66
67      m = length(t_exp_MEA);
68
69      %MEA
70      abs_err_MEA = zeros(1,m);
71      rel_err_MEA = zeros(1,m);
72      y_mod_MEA = y_mod(:,1);
73      y_mod_ip_MEA = interp1(tspan,y_mod_MEA',t_exp_MEA,'linear');
74
75      %HEEDA
76      abs_err_HEEDA = zeros(1,m);
77      rel_err_HEEDA = zeros(1,m);
78      y_mod_HEEDA = y_mod(:,2);
79      y_mod_ip_HEEDA = interp1(tspan,y_mod_HEEDA',t_exp_MEA,'linear');
80
81      %Trimer
82      abs_err_Trimer = zeros(1,m);
83      rel_err_Trimer = zeros(1,m);
84      y_mod_Trimer = y_mod(:,3);
85      y_mod_ip_Trimer = interp1(tspan,y_mod_Trimer',t_exp_MEA,'linear');
86
87      %HEIA
88      abs_err_HEIA = zeros(1,m);
89      rel_err_HEIA = zeros(1,m);
90      y_mod_HEIA = y_mod(:,5);
91      y_mod_ip_HEIA = interp1(tspan,y_mod_HEIA',t_exp_MEA,'linear');
92
93      %triHEIA
94      abs_err_triHEIA = zeros(1,m);
95      rel_err_triHEIA = zeros(1,m);
96      y_mod_triHEIA = y_mod(:,6);
97      y_mod_ip_triHEIA = interp1(tspan,y_mod_triHEIA',t_exp_MEA,'linear');
98
```

```
99      count = 0;
100
101     %Fill in errors for each experimental point at the right place in the
102     %error arrays for each component and for the complete model
103
104     %MEA
105     for j = 1:m
106         abs_err_MEA(j) = y_mod_ip_MEA(j) - y_exp_MEA(j);
107         abs_err_mod_MEA(count3 + j) = abs_err_MEA(j);
108         abs_err_tot(count2 + j) = abs_err_MEA(j);
109
110         rel_err_MEA(j) = (y_mod_ip_MEA(j)-y_exp_MEA(j))/ y_exp_MEA(j);
111         rel_err_mod_MEA(count3 + j) = rel_err_MEA(j);
112         rel_err_tot(count2 + j) = rel_err_MEA(j);
113
114         T_tot(count2 + j) = T;
115         T_comp(count3 + j) = T;
116         load_tot(count2 + j) = CO2_load;
117         load_comp(count3 + j) = CO2_load;
118         time_tot(count2 + j) = t_exp_MEA(j);
119         time_comp(count3 + j) = t_exp_MEA(j);
120         exp_tot(count2 + j) = y_exp_MEA(j);
121         exp_comp_MEA(count3 + j) = y_exp_MEA(j);
122
123     end
124
125     count = count + m;
126
127     %HEEDA
128     for j = 1:m
129         abs_err_HEEDA(j) = y_mod_ip_HEEDA(j) - y_exp_HEEDA(j);
130         abs_err_mod_HEEDA(count3 + j) = abs_err_HEEDA(j);
131         abs_err_tot(count2 + j) = abs_err_HEEDA(j);
132
133         rel_err_HEEDA(j) = (y_mod_ip_HEEDA(j)-y_exp_HEEDA(j))/ y_exp_HEEDA(j); %
134         rel_err_mod_HEEDA(count3 + j) = rel_err_HEEDA(j);
135         rel_err_tot(count2 + count + j) = rel_err_HEEDA(j);
136
137         T_tot(count2+ count + j) = T;
138         load_tot(count2+ count + j) = CO2_load;
139         time_tot(count2 + count + j) = t_exp_MEA(j);
140         exp_tot(count2 + count+ j) = y_exp_HEEDA(j);
141         exp_comp_HEEDA(count3 + j) = y_exp_HEEDA(j);
142     end
143
144     count = count + m;
145
146     %Trimer
```

```
147     for j = 1:m
148         abs_err_Trimer(j) = y_mod_ip_Trimer(j) - y_exp_Trimer(j);
149         abs_err_mod_Trimer(count3 + j) = abs_err_Trimer(j);
150         abs_err_tot(count2 + count + j) = abs_err_Trimer(j);
151 
152         rel_err_Trimer(j) = (y_mod_ip_Trimer(j)-y_exp_Trimer(j))/ y_exp_Trimer(j)
                ; %
153         rel_err_mod_Trimer(count3 + j) = rel_err_Trimer(j);
154         rel_err_tot(count2 + count + j) = rel_err_Trimer(j);
155 
156         T_tot(count2+ count + j) = T;
157         load_tot(count2+ count + j) = CO2_load;
158         time_tot(count2 + j) = t_exp_MEA(j);
159         exp_tot(count2 + count+ j) = y_exp_Trimer(j);
160         exp_comp_trimer(count3 + j) = y_exp_Trimer(j);
161     end
162 
163     count = count + m;
164 
165     %HEIA
166     for j = 1:m
167         abs_err_HEIA(j) = y_mod_ip_HEIA(j) - y_exp_HEIA(j);
168         abs_err_mod_HEIA(count3 + j) = abs_err_HEIA(j);
169         abs_err_tot(count2 + count + j) = abs_err_HEIA(j);
170 
171         rel_err_HEIA(j) = (y_mod_ip_HEIA(j)-y_exp_HEIA(j))/ y_exp_HEIA(j); %
172         rel_err_mod_HEIA(count3 + j) = rel_err_HEIA(j);
173         rel_err_tot(count2 + count + j) = rel_err_HEIA(j);
174 
175         T_tot(count2+ count + j) = T;
176         load_tot(count2+ count + j) = CO2_load;
177         time_tot(count2+ count + j) = t_exp_MEA(j);
178         exp_tot(count2 + count+ j) = y_exp_HEIA(j);
179         exp_comp_HEIA(count3 + j) = y_exp_HEIA(j);
180     end
181 
182     count = count + m;
183 
184     %TriHEIA
185     for j = 1:m
186         abs_err_triHEIA(j) = y_mod_ip_triHEIA(j) - y_exp_triHEIA(j);
187         abs_err_mod_triHEIA(count3 + j) = abs_err_triHEIA(j);
188         abs_err_tot(count2 + count + j) = abs_err_triHEIA(j);
189 
190         rel_err_triHEIA(j) = (y_mod_ip_triHEIA(j)-y_exp_triHEIA(j))/
                y_exp_triHEIA(j); %
191         rel_err_mod_triHEIA(count3 + j) = rel_err_triHEIA(j);
192         rel_err_tot(count2 + count + j) = rel_err_triHEIA(j);
```

```
193
194             T_tot(count2+ count + j) = T;
195             load_tot(count2+ count + j) = CO2_load;
196             time_tot(count2 + j) = t_exp_MEA(j);
197             exp_tot(count2 + count+ j) = y_exp_HEEDA(j);
198             exp_comp_triHEIA(count3 + j) = y_exp_triHEIA(j);
199         end
200
201         count2 = count2 + 5*m;
202         count3 = count3 + m;
203     end
204
205     abs_err_mod_MEA_nonzero = abs_err_mod_MEA(abs_err_mod_MEA~=0); % for
            investigating errors without the first points in each exp
206
207     %% Use only the availible experimental data (where the exp values are not only
            zero)
208     % (This was done manually, should be changed similar to objective function)
209
210     abs_err_mod_HEEDA_val = abs_err_mod_HEEDA(1:89);
211     T_comp_HEEDA = T_comp(1:89);
212     load_comp_HEEDA = load_comp(1:89);
213     time_comp_HEEDA = time_comp(1:89);
214     abs_err_mod_HEEDA_nonzero = abs_err_mod_HEEDA_val(abs_err_mod_HEEDA_val~=0);
215
216     abs_err_mod_Trimer_val = abs_err_mod_Trimer(1:37);
217     T_comp_Trimer = T_comp(1:37);
218     load_comp_Trimer = load_comp(1:37);
219     time_comp_Trimer = time_comp(1:37);
220     abs_err_mod_Trimer_nonzero = abs_err_mod_Trimer_val(abs_err_mod_Trimer_val~=0);
221
222     abs_err_mod_HEIA_val = abs_err_mod_HEIA(1:89);
223     T_comp_HEIA = T_comp(1:89);
224     load_comp_HEIA = load_comp(1:89);
225     time_comp_HEIA = time_comp(1:89);
226     abs_err_mod_HEIA_nonzero = abs_err_mod_HEIA_val(abs_err_mod_HEIA_val~=0);
227
228     abs_err_mod_triHEIA_val = abs_err_mod_triHEIA(17:37);
229     T_comp_triHEIA = T_comp(17:37);
230     load_comp_triHEIA = load_comp(17:37);
231     time_comp_triHEIA = time_comp(17:37);
232     abs_err_mod_triHEIA_nonzero = abs_err_mod_triHEIA_val(abs_err_mod_triHEIA_val~=0)
            ;
233
234     %% Find average abs and rel error for all comp
235     av_abs_err = zeros(1,5);
236     av_abs_err(1) = mean(abs_err_mod_MEA);
237     av_abs_err(2) = mean(abs_err_mod_HEEDA_val);
```

```
av_abs_err(3) = mean(abs_err_mod_Trimer_val);
av_abs_err(4) = mean(abs_err_mod_HEIA_val);
av_abs_err(5) = mean(abs_err_mod_triHEIA_val);

av_abs_err_nonzero = zeros(1,5);
av_abs_err_nonzero(1) = mean(abs_err_mod_MEA_nonzero);
av_abs_err_nonzero(2) = mean(abs_err_mod_HEEDA_nonzero);
av_abs_err_nonzero(3) = mean(abs_err_mod_Trimer_nonzero);
av_abs_err_nonzero(4) = mean(abs_err_mod_HEIA_nonzero);
av_abs_err_nonzero(5) = mean(abs_err_mod_triHEIA_nonzero);

abs_av_abs_err = zeros(1,5);
abs_av_abs_err(1) = mean(abs(abs_err_mod_MEA));
abs_av_abs_err(2) = mean(abs(abs_err_mod_HEEDA_val));
abs_av_abs_err(3) = mean(abs(abs_err_mod_Trimer_val));
abs_av_abs_err(4) = mean(abs(abs_err_mod_HEIA_val));
abs_av_abs_err(5) = mean(abs(abs_err_mod_triHEIA_val));

abs_av_abs_err_nonzero = zeros(1,5);
abs_av_abs_err_nonzero(1) = mean(abs(abs_err_mod_MEA));
abs_av_abs_err_nonzero(2) = mean(abs(abs_err_mod_HEEDA_nonzero));
abs_av_abs_err_nonzero(3) = mean(abs(abs_err_mod_Trimer_nonzero));
abs_av_abs_err_nonzero(4) = mean(abs(abs_err_mod_HEIA_nonzero));
abs_av_abs_err_nonzero(5) = mean(abs(abs_err_mod_triHEIA_nonzero));

%Remove Nan from rel lists
rel_err_mod_MEA(isnan(rel_err_mod_MEA))=[];
rel_err_mod_HEEDA(isnan(rel_err_mod_HEEDA))=[];
rel_err_mod_Trimer(isnan(rel_err_mod_Trimer))=[];
rel_err_mod_HEIA(isnan(rel_err_mod_HEIA))=[];
rel_err_mod_triHEIA(isnan(rel_err_mod_triHEIA))=[];

%Remove inf from lists
rel_err_mod_MEA(isinf( rel_err_mod_MEA ))=[];
rel_err_mod_HEEDA(isinf( rel_err_mod_HEEDA ))=[];
rel_err_mod_Trimer(isinf( rel_err_mod_Trimer ))=[];
rel_err_mod_HEIA(isinf( rel_err_mod_HEIA ))=[];
rel_err_mod_triHEIA(isinf( rel_err_mod_triHEIA ))=[];

av_rel_err = zeros(1,5);
av_rel_err(1) = mean(rel_err_mod_MEA);
av_rel_err(2) = mean(rel_err_mod_HEEDA);
av_rel_err(3) = mean(rel_err_mod_Trimer);
av_rel_err(4) = mean(rel_err_mod_HEIA);
av_rel_err(5) = mean(rel_err_mod_triHEIA);

abs_av_rel_err = zeros(1,5);
abs_av_rel_err(1) = mean(abs(rel_err_mod_MEA));
```

```
abs_av_rel_err(2) = mean(abs(rel_err_mod_HEEDA));
abs_av_rel_err(3) = mean(abs(rel_err_mod_Trimer));
abs_av_rel_err(4) = mean(abs(rel_err_mod_HEIA));
abs_av_rel_err(5) = mean(abs(rel_err_mod_triHEIA));

rel_err_mod_MEA_nonzero = rel_err_mod_MEA(rel_err_mod_MEA~=0);
rel_err_mod_HEEDA_nonzero = rel_err_mod_HEEDA(rel_err_mod_HEEDA~=0);
rel_err_mod_Trimer_nonzero = rel_err_mod_Trimer(rel_err_mod_Trimer~=0);
rel_err_mod_HEIA_nonzero = rel_err_mod_HEIA(rel_err_mod_HEIA~=0);
rel_err_mod_triHEIA_nonzero = rel_err_mod_triHEIA(rel_err_mod_triHEIA~=0);

av_rel_err_nonzero = zeros(1,5);
av_rel_err_nonzero(1) = mean(rel_err_mod_MEA_nonzero);
av_rel_err_nonzero(2) = mean(rel_err_mod_HEEDA_nonzero);
av_rel_err_nonzero(3) = mean(rel_err_mod_Trimer_nonzero);
av_rel_err_nonzero(4) = mean(rel_err_mod_HEIA_nonzero);
av_rel_err_nonzero(5) = mean(rel_err_mod_triHEIA_nonzero);

abs_av_rel_err_nonzero = zeros(1,5);
abs_av_rel_err_nonzero(1) = mean(abs(rel_err_mod_MEA_nonzero));
abs_av_rel_err_nonzero(2) = mean(abs(rel_err_mod_HEEDA_nonzero));
abs_av_rel_err_nonzero(3) = mean(abs(rel_err_mod_Trimer_nonzero));
abs_av_rel_err_nonzero(4) = mean(abs(rel_err_mod_HEIA_nonzero));
abs_av_rel_err_nonzero(5) = mean(abs(rel_err_mod_triHEIA_nonzero));

%% The abs errors from Davis' Model
abs_err_Davis_MEA = [0    -0.1083         0    0.1491         0    0.2200
    0    0.3736         0    0.2230         0    0.3034
                   0    0.3026         0    0.2279         0    0.1037    0.0270
       0.1461    0.1604    0.0821         0    0.0464
            0.0428    0.0295    0.0846    0.0793         0    0.0578    0.0773
    0.0648   -0.0432         0    0.0250    0.0172
            0.0208         0    0.0173   -0.0198    0.4387    0.4147    0.4169
            0    0.2406         0    0.2207         0
            0.2166         0    0.0366         0   -0.2113         0   -0.0656
            0   -0.3679         0   -0.6057         0
           -0.4977         0   -2.2075         0   -0.0801         0   -0.8826
    -1.1143   -1.0674         0   -1.2001   -0.7903
           -0.1584         0   -0.0075   -0.0923   -0.1006         0   -0.2528
    -0.2999   -0.2511         0   -0.0295   -0.0380
            0.2470    0.4065    0.3761         0   -0.0449   -0.2079   -0.4657
    -0.5464   -0.6693         0    0.0986    0.0978
            0.1894    0.1054    0.1544         0   -0.0342    0.0058    0.2377
    0.1105    0.0382         0    0.0041    0.4641         0.3114    0.0784
    0.1331         0   -0.2043                                        ];
abs_err_Davis_HEEDA = [0    -0.0469         0   -0.0248         0   -0.0209
            0    0.0038         0   -0.0012         0    0.0135
                   0    0.0261         0   -0.0109         0   -0.0117   -0.0256
```

```
    -0.0186   -0.0010    0.0248         0    0.0196
          -0.0067   -0.0145   -0.0038    0.0414         0    0.0077    0.0057
     0.0061    0.0106         0   -0.0014   -0.0024
          -0.0108         0   -0.0867   -0.0840   -0.0735   -0.0417   -0.0273
          0    0.0188         0    0.0348         0
          0.0417         0    0.0975         0    0.1111         0    0.1125
          0    0.0235         0    0.0390         0
          0.0582         0    0.0652         0    0.0328         0    0.1987
 0.1937   -0.0685         0    0.0042   -0.0615
          -0.2550         0    0.0370    0.0645    0.0648         0    0.0930
     0.0999    0.1051         0   -0.0264   -0.0506
          -0.0619   -0.0186   -0.0154         0    0.0553
                    ];
abs_err_Davis_Trimer = [0   -0.0028         0   -0.0030         0   -0.0112
          0    0.0011         0    0.0070         0 0.0004         0   -0.0054
          0   -0.0048         0    0.0087    0.0050   -0.0023   -0.0040
 0.0009 0    0.0005   -0.0026   -0.0026   -0.0077   -0.0040         0   -0.0038
    -0.0041   -0.0085   -0.0131 0    0.0003    0.0014   -0.0064];
abs_err_Davis_HEIA = [0    0.0072         0   -0.0160         0   -0.0025
          0    0.0030         0   -0.1590         0   -0.1780
                    0   -0.1271         0   -0.0437         0   -0.0069   -0.0535
    -0.0513   -0.0814    0.0345         0    0.0330
          -0.0034   -0.0212    0.0232    0.0508         0    0.0188    0.0089
 -0.0231    0.0110         0    0.0009    0.0039
          0.0110         0   -0.0726   -0.1883   -0.2878   -0.2437   -0.2478
          0   -0.0191         0   -0.0307         0
          -0.0291         0   -0.0430         0   -0.1775         0   -0.0777
          0    0.1389         0    0.1424         0
          0.2488         0    0.5434         0    0.0017         0    0.4189
 0.1035   -1.0680         0    0.4734    0.1029
          -1.7328         0    0.0051   -0.0570   -0.1346         0    0.0721
     0.1452    0.1913         0    0.0010   -0.0550
          -0.1494   -0.0757   -0.0879         0    0.0073
                    ];
abs_err_Davis_triHEIA = [0    0.0141         0    0.0072         0    0.0084
          0    0.0001         0   -0.0082         0 -0.0239         0   -0.0316
          0    0.0008         0   -0.0023    0.0019   -0.0047   -0.0162
 -0.0471 0   -0.0031    0.0050    0.0012   -0.0154   -0.0781         0
 -0.0011    0.0010    0.0017   -0.0065 0   -0.0008   -0.0004   -0.0009];

%% plotting the abs error for each component in the model towards Davis' Model
figure(1000);
plot(0.8,abs_err_Davis_MEA,'x','color', [0.7 0.7 0.7]);
hold on;
plot(1,abs_err_mod_MEA,'x','color', [0.6350 0.0780 0.1840]);
hold on;
plot(1.8,abs_err_Davis_HEEDA,'x','color', [0.7 0.7 0.7]);
hold on;
```

```
plot(2,abs_err_mod_HEEDA_val,'x','color', [0.4940 0.1840 0.5560]);
hold on;
plot(2.8,abs_err_Davis_Trimer,'x','color', [0.7 0.7 0.7]);
hold on;
plot(3,abs_err_mod_Trimer_val,'x','color', [0.9290, 0.6940, 0.1250]);
hold on;
plot(3.8,abs_err_Davis_HEIA,'x','color', [0.7 0.7 0.7]);
hold on;
plot(4,abs_err_mod_HEIA_val,'x','color', [0 0.4470 0.7410]);
hold on;
plot(4.8,abs_err_Davis_triHEIA,'x','color', [0.7 0.7 0.7]);
hold on;
plot(5,abs_err_mod_triHEIA_val,'x','color', [0.4660, 0.6740, 0.1880]);

xticks([0.8 1.8 2.8 3.8 4.8])
xticklabels({'MEA','HEEDA','Trimer','HEIA','triHEIA'})
ylim([-2.5,2.5])
xlim([-0 5.8])
yline(0);
hold off;

%% The rel errors from Davis' Model
figure(2000);
rel_err_Davis_MEA = [0    -0.0290          0    0.0391          0    0.0557
    0    0.0830          0    0.0708          0    0.0908
                   0    0.0865          0    0.0509          0    0.0251    0.0074
       0.0516    0.0652    0.0446          0    0.0101
            0.0102    0.0076    0.0277    0.0415          0    0.0124    0.0175
    0.0164   -0.0123          0    0.0051    0.0036
            0.0044          0    0.0047   -0.0060    0.1783    0.1920    0.2217
            0    0.0515          0    0.0477          0
            0.0473          0    0.0082          0   -0.0491          0   -0.0166
            0   -0.1009          0   -0.2215          0
            -0.2270          0   -1.0070          0   -0.0167          0   -0.3074
    -0.4534   -1.0675          0   -0.6606   -0.8881
            -1.2817          0   -0.0016   -0.0193   -0.0215          0   -0.0589
    -0.0822   -0.0817          0   -0.0069   -0.0103
            0.0843    0.1712    0.1816          0   -0.0092   -0.0426   -0.0930
    -0.1099   -0.1344          0    0.0212    0.0223
            0.0468    0.0270    0.0422          0   -0.0076    0.0014    0.0672
    0.0327    0.0119          0    0.0009    0.1373
            0.0995    0.0259    0.0499          0   -0.0673
                    ];
rel_err_Davis_HEEDA = [-0.2040   -0.1303   -0.1230    0.1266   -0.0078    0.0964
       0.2174   -0.1365   -0.0729   -0.1349   -0.1031   -0.0064
                                  0.1911    0.2456   -0.0449   -0.0853   -0.0235
        0.3764    0.1098    0.0520    0.0436    0.0758   -0.0700   -0.0600
                                           -0.1543   -0.4279   -0.3868   -0.3559
```

```
    -0.2427   -0.1763    4.8731    3.3673    3.4087    0.1427    0.3452
   0.7968                                                0.7416    4.4232    4.9262
   -0.6031    0.0326   -0.4146   -0.9824    4.9352    5.4690    1.8933    1.5505
     1.6929                                                2.0607   -0.1581
   -0.2478   -0.2926   -0.1138   -0.0986   -0.1464
                  0.0582         0    0.0652         0    0.0328         0
   0.1987    0.1937   -0.0685         0    0.0042   -0.0615
                           -0.2550         0    0.0370    0.0645    0.0648
           0    0.0930    0.0999    0.1051         0   -0.0264   -0.0506
                                          -0.0619   -0.0186   -0.0154         0
     0.0553                                                ];
rel_err_Davis_Trimer = [0   -0.0555         0   -0.0760         0   -0.2790
           0         0    0.1761         0    0.0107  0   -0.1346         0
   -0.4815         0    0.4365    0.1251   -0.0451   -0.0794    0.0229         0
   0.0451   -0.0858   -0.0656   -0.1546   -0.0997         0   -0.3836   -0.2051
     -0.2116   -0.2618         0  -0.6375];
rel_err_Davis_HEIA = [0.0286   -0.0802   -0.0179   -0.3179   -0.3956   -0.3531
   -0.7286   -0.0573   -0.1672   -0.1046   -0.1357    0.0565
                                  -0.0284   -0.0924    0.0610    0.0876
   0.1783   -0.1155    0.0356   -0.4835   -0.4926   -0.4935   -0.3925   -0.3591
                                             -0.9564   -0.9033   -0.8544
   -0.4300   -0.5284   -0.2699    0.7468    0.3049    0.5351    0.0990   18.4442
     0.3090                                               -0.8396    2.2529
   0.2162   -0.9603   -0.7589   -0.7867    0.8008    0.7333    0.6858    0.0094
     -0.1702   -0.2738                                              -0.1325
   -0.1330    0.7938                                                ];
rel_err_Davis_triHEIA = [0    0.4698         0    0.3587         0    0.8361
           0         0   -0.1170         0   -0.3418  0   -0.4518         0
           0    -0.1641    0.0472   -0.0491   -0.1226   -0.2253         0
   -0.6122  0.6299    0.0390   -0.1590   -0.3339         0   -0.5470    0.2548
   0.0695   -0.0973         0   -0.9872  -0.8014   -0.6515];

%% plotting the rel error for each component in the model towards Davis' Model
plot(0,rel_err_Davis_MEA,'x','color', [0.7  0.7  0.7]);
hold on;
plot(2,rel_err_mod_MEA,'x','color', [0.6350  0.0780  0.1840]);
hold on;
plot(15,rel_err_Davis_HEEDA,'x','color', [0.7  0.7  0.7]);
hold on;
plot(17,rel_err_mod_HEEDA,'x','color', [0.4940  0.1840  0.5560]);
hold on;
plot(30,rel_err_Davis_Trimer,'x','color', [0.7  0.7  0.7]);
hold on;
plot(32,rel_err_mod_Trimer,'x','color', [0.9290, 0.6940, 0.1250]);
hold on;
plot(45,rel_err_Davis_HEIA,'x','color', [0.7  0.7  0.7]);
hold on;
plot(47,rel_err_mod_HEIA,'x','color', [0  0.4470  0.7410]);
```

```
hold on;
plot(60,rel_err_Davis_triHEIA,'x','color', [0.7 0.7 0.7]);
hold on;
plot(62,rel_err_mod_triHEIA,'x','color', [0.4660, 0.6740, 0.1880]);

xticks([0 15 30 45 60])
xticklabels({'MEA','HEEDA','Trimer','HEIA','triHEIA'})
ylim([-5,25])
xlim([-10 72])
yline(0);
hold off;


%% Plotting abs errors for each components at the different stripper conditions

%MEA
figure(3000);
title('MEA')
h(1) =subplot(2,2,1) ;
plot(T_comp,abs_err_mod_MEA,'x','color', [0.6350 0.0780 0.1840])
yline(0);
xlabel('Temperature')
h(2) = subplot(2,2,2);
plot(load_comp,abs_err_mod_MEA,'x','color', [0.6350 0.0780 0.1840])
xlabel('CO2 loading')
yline(0);
h(3) = subplot(2,2,3);
plot(time_comp,abs_err_mod_MEA,'x','color', [0.6350 0.0780 0.1840])
yline(0);
xlabel('Time')
pos = get(h,'Position');
new = mean(cellfun(@(v)v(1),pos(1:2)));
set(h(3),'Position',[new,pos{end}(2:end)])
sgt = sgtitle('MEA');
sgt.FontSize = 12;

%HEEDA
figure(4000);
h(1) =subplot(2,2,1) ;
plot(T_comp_HEEDA,abs_err_mod_HEEDA_val,'x','color', [0.4940 0.1840 0.5560])
yline(0);
xlabel('Temperature')
h(2) = subplot(2,2,2);
plot(load_comp_HEEDA,abs_err_mod_HEEDA_val,'x','color', [0.4940 0.1840 0.5560])
yline(0);
xlabel('CO2 loading')
h(3) = subplot(2,2,3);
plot(time_comp_HEEDA,abs_err_mod_HEEDA_val,'x','color', [0.4940 0.1840 0.5560])
```

```
yline(0);
xlabel('Time')
pos = get(h,'Position');
new = mean(cellfun(@(v)v(1),pos(1:2)));
set(h(3),'Position',[new,pos{end}(2:end)])
sgt = sgtitle('HEEDA');
sgt.FontSize = 12;

%Trimer
figure(5000);
h(1) =subplot(2,2,1) ;
plot(T_comp_Trimer,abs_err_mod_Trimer_val,'x','color', [0.9290, 0.6940, 0.1250])
yline(0);
xlabel('Temperature')
h(2) = subplot(2,2,2);
plot(load_comp_Trimer,abs_err_mod_Trimer_val,'x','color', [0.9290, 0.6940,
    0.1250])
yline(0);
xlabel('CO2 loading')
h(3) = subplot(2,2,3);
plot(time_comp_Trimer,abs_err_mod_Trimer_val,'x','color', [0.9290, 0.6940,
    0.1250])
yline(0);
xlabel('Time')
pos = get(h,'Position');
new = mean(cellfun(@(v)v(1),pos(1:2)));
set(h(3),'Position',[new,pos{end}(2:end)])
sgt = sgtitle('Trimer');
sgt.FontSize = 12;

%HEIA
figure(6000);
h(1) =subplot(2,2,1) ;
plot(T_comp_HEIA,abs_err_mod_HEIA_val,'x','color', [0 0.4470 0.7410])
yline(0);
xlabel('Temperature')
h(2) = subplot(2,2,2);
plot(load_comp_HEIA,abs_err_mod_HEIA_val,'x','color', [0 0.4470 0.7410])
yline(0);
xlabel('CO2 loading')
h(3) = subplot(2,2,3);
plot(time_comp_HEIA,abs_err_mod_HEIA_val,'x','color', [0 0.4470 0.7410])
yline(0);
xlabel('Time')
pos = get(h,'Position');
new = mean(cellfun(@(v)v(1),pos(1:2)));
set(h(3),'Position',[new,pos{end}(2:end)])
sgt = sgtitle('HEIA');
```

```
sgt.FontSize = 12;

%TriHEIA
figure(7000);
h(1) =subplot(2,2,1) ;
plot(T_comp_triHEIA,abs_err_mod_triHEIA_val,'x','color', [0.4660, 0.6740,
    0.1880])
yline(0);
xlabel('Temperature')
h(2) = subplot(2,2,2);
plot(load_comp_triHEIA,abs_err_mod_triHEIA_val,'x','color', [0.4660, 0.6740,
    0.1880])
yline(0);
xlabel('CO2 loading')
h(3) = subplot(2,2,3);
plot(time_comp_triHEIA,abs_err_mod_triHEIA_val,'x','color', [0.4660, 0.6740,
    0.1880])
yline(0);
xlabel('Time')
pos = get(h,'Position');
new = mean(cellfun(@(v)v(1),pos(1:2)));
set(h(3),'Position',[new,pos{end}(2:end)])
sgt = sgtitle('TriHEIA');
sgt.FontSize = 12;

end
```

G.13 Auxiliary Plotting function 1

```
%PLOTTING y_mod vs y_exp
function plotting_mod(tspan, y_mod, t_exp_MEA, y_exp_MEA, y_exp_HEEDA, y_exp_HEIA
    , y_exp_Trimer, y_exp_triHEIA, T, CO2_load)

%txt = ['T = ' num2str(T) ', CO2 load = ' num2str(CO2_load)];
%title(txt);
ylim([0 5]);
t_end = t_exp_MEA(end);
xlim([-0 t_end + 0.1])
grid on
hold on;

%Make legend using dummy points
x1 = 0;
x2 = 0;
x3 = 0;
x4 = 0;
x5 = 0;
y = 0;
```

```
19
20 plot(x1, y,'s','color',[0.6350 0.0780 0.1840],'LineWidth',1,'MarkerFaceColor'
       ,[0.6350 0.0780 0.1840])
21 plot(x2, y,'s','color',[0.4940 0.1840 0.5560],'LineWidth',1,'MarkerFaceColor'
       ,[0.4940 0.1840 0.5560])
22 plot(x3, y,'s','color',[0.9290, 0.6940, 0.1250],'LineWidth',1,'MarkerFaceColor'
       ,[0.9290, 0.6940, 0.1250])
23 plot(x4, y,'s','color',[0 0.4470 0.7410],'LineWidth',1,'MarkerFaceColor',[0
       0.4470 0.7410])
24 plot(x5, y,'s','color',[0.4660, 0.6740, 0.1880],'LineWidth',1,'MarkerFaceColor'
       ,[0.4660, 0.6740, 0.1880])
25 hold off;
26 legend({'MEA','HEEDA','Trimer','HEIA','triHEIA'},'Location','best');
27 %lgd.FontSize = 7;
28 hold on;
29
30 set(groot,'defaultLegendAutoUpdate','off');
31 yyaxis right  %MEA only
32 ylim([0 5]);
33 xlim([-0 t_end + 0.1])
34
35
36 if all(y_exp_MEA == y_exp_MEA(1))
37 else
38     plot(tspan,y_mod(:,1),'-','color',[0.6350 0.0780 0.1840],'LineWidth',1); %MEA
39     hold on
40     plot(t_exp_MEA,y_exp_MEA,'s','MarkerEdgeColor',[0.6350 0.0780 0.1840],'
           LineWidth',1)
41     hold on
42 end
43
44
45 yyaxis left
46 ylim([0 2.5])
47
48 %Only plot if the experimental values are different from zero
49
50 %HEEDA
51 if all(y_exp_HEEDA == y_exp_HEEDA(1))
52 else
53     plot(tspan,y_mod(:,2),'-','color', [0.4940 0.1840 0.5560],'LineWidth',1)
54     hold on
55     plot(t_exp_MEA,y_exp_HEEDA,'^','MarkerEdgeColor',[0.4940 0.1840 0.5560],'
           LineWidth',1)
56     hold on
57 end
58
59 %Trimer
```

```
if all(y_exp_Trimer == y_exp_Trimer(1))
else
    plot(tspan,y_mod(:,3),'-','color',[0.9290, 0.6940, 0.1250],'LineWidth',1)
    hold on
    plot(t_exp_MEA,y_exp_Trimer,'o','MarkerEdgeColor',[0.9290, 0.6940, 0.1250],'
        LineWidth',1)
    hold on
end

%HEIA
if all(y_exp_HEIA == y_exp_HEIA(1))
else
    plot(tspan,y_mod(:,5),'-','color',[0 0.4470 0.7410],'LineWidth',1)
    hold on
    plot(t_exp_MEA,y_exp_HEIA,'d','MarkerEdgeColor',[0 0.4470 0.7410],'LineWidth'
        ,1)
    hold on
end

%TriHEIA
if all(y_exp_triHEIA == y_exp_triHEIA(1))
else
    plot(tspan,y_mod(:,6),'-','color',[0.4660, 0.6740, 0.1880],'LineWidth',1)
    hold on
    plot(t_exp_MEA,y_exp_triHEIA,'d','MarkerEdgeColor',[0.4660, 0.6740, 0.1880],'
        LineWidth',1)
    hold on
end

hold off;
end
```

G.14 Auxiliary Plotting function 2

```
function plot_par(e_MEA, e_HEEDA, e_Trimer, e_triHEIA, e_HEIA, parameter)
    plot(parameter, e_MEA, 'x');
    hold on;
    plot(parameter, e_HEEDA, 'x');
    hold on;
    plot(parameter, e_Trimer, 'x');
    hold on;
    plot(parameter, e_triHEIA, 'x');
    hold on;
    plot(parameter, e_HEIA, 'x');
    hold on;
end
```

NTNU
Norwegian University of
Science and Technology